Proceedings of the Royal Society of Edinburgh, page 1 of 40
DOI:10.1017/prm.2024.24

Bifurcations and pattern formation in a host–parasitoid model with nonlocal effect

Chuang Xiang
School of Mathematical Sciences, Nanjing Normal University, Nanjing 210023, P. R. China (1604059603@qq.com)
School of Mathematics and Statistics, Central China Normal University, Wuhan, Hubei 430079, P. R. China

Jicai Huang and Min Lu
School of Mathematics and Statistics, Central China Normal University, Wuhan, Hubei 430079, P. R. China (hjc@ccnu.edu.cn, lumin@mails.ccnu.edu.cn)

Shigui Ruan
Department of Mathematics, University of Miami, Coral Gables, FL 33146, USA (ruan@math.miami.edu)

Hao Wang
Department of Mathematical and Statistical Sciences, University of Alberta, Edmonton, AB T6G 2G1, Canada (hao8@ualberta.ca)

(Received 26 August 2023; accepted 5 February 2024)

In this paper, we analyse Turing instability and bifurcations in a host–parasitoid model with nonlocal effect. For a ordinary differential equation model, we provide some preliminary analysis on Hopf bifurcation. For a reaction–diffusion model with local intraspecific prey competition, we first explore the Turing instability of spatially homogeneous steady states. Next, we show that the model can undergo Hopf bifurcation and Turing–Hopf bifurcation, and find that a pair of spatially nonhomogeneous periodic solutions is stable for a *(8,0)-mode Turing–Hopf bifurcation* and unstable for a *(3,0)-mode Turing–Hopf bifurcation*. For a reaction–diffusion model with nonlocal intraspecific prey competition, we study the existence of the Hopf bifurcation, double-Hopf bifurcation, Turing bifurcation, and Turing–Hopf bifurcation successively, and find that a spatially nonhomogeneous quasi-periodic solution is unstable for a *(0,1)-mode double-Hopf bifurcation*. Our results indicate that the model exhibits complex pattern formations, including transient states, monostability, bistability, and tristability. Finally, numerical simulations are provided to illustrate complex dynamics and verify our theoretical results.

Keywords: host–parasitoid model; Turing instability; Hopf bifurcation; Turing–Hopf bifurcation; double-Hopf bifurcation; pattern formation

2010 *Mathematics Subject Classification:* 34C23; 35K57; 92D25

1. Introduction

Many kinds of predator–prey systems have been developed, refined and widely studied since the Lotka–Volterra system was proposed and analysed, but most of these studies considered specialist predators [9, 27] that rely on a single-prey species to survive and will go extinct in the absence of the prey. However, in the real world, many predators have several alternative prey species as food and can persist by switching to other food sources even when one desired prey species is scarce. Such predators are called generalist predators, such as foxes, common buzzards, cats, etc. Recently, there are some works considering generalist predators (see [9, 11, 17, 21, 23, 26, 30, 35, 38–40] and references therein). Comparing to predator–prey systems with specialist predators, predator–prey systems with generalist predators can undergo richer dynamical behaviours and bifurcation phenomena [9, 31, 38–40].

One main method to incorporate generalist predation in predator–prey systems is to assume that alternative resources are constant and the predator's equation is logistic or logistic-like form in the absence of the prey (see [9, 23, 26, 38, 39] and references therein). For example, in order to explore factors to stop and even sometimes to reverse the invasion of lepidopteron, Magal *et al.* [26] developed the following host (prey)–parasitoid (generalist predators) diffusive model:

$$\begin{cases} \dfrac{\partial u}{\partial t} = D\Delta u + r_1 u\left(1 - \dfrac{u}{K_1}\right) - \dfrac{Euv}{1+Ehu}, \\ \dfrac{\partial v}{\partial t} = D\Delta v + r_2 v\left(1 - \dfrac{v}{K_2}\right) + \dfrac{\gamma Euv}{1+Ehu}, \end{cases} \tag{1.1}$$

where $u(x, t)$ and $v(x, t)$ stand for the densities of the hosts (prey) and parasitoids (generalist predators) at location $x \in \Omega$ and time $t \geqslant 0$, respectively. The parameter D represents the diffusion rate, r_1 is the growth rate of hosts, r_2 describes the growth rate of parasitoids, K_1 is the carrying capacity of hosts and K_2 denote the carrying capacity of parasitoids in the absence of hosts, E is the encounter rate of hosts and parasitoids, γ is the conversion rate of parasitoids, and h describes the harvesting time. In system (1.1), when $u(x, t) = 0$, the predators can still survive with logistic growth. Under Neumann boundary condition, Magal *et al.* [26] performed numerical simulations, such as the existence of travelling waves, to identify the conditions for which the leafminers advance can be stopped and reversed by parasitoids. By considering different diffusion rates for predator and prey, Madec *et al.* [25] found that bistability induced by generalist natural enemies can reverse pest invasions. Du and Lou [8] also studied the existence and nonexistence of non-constant positive steady states under different diffusion rates. A wealth of conclusions about system (1.1) are obtained, but the detailed theoretical analysis is not complete.

In studying spatiotemporal dynamics for single and multiple interacting components, it is usually assumed that individuals only interact with their nearby neighbours, which is often termed local interactions [4]. Furter and Grinfeld [12] claimed that it is untenable to assume plainly that the interactions among individuals are always local, as organisms may tend to communicate with their peers in certain ranges, which causes nonlocal interactions. Ermentrout and Cowan [10] showed that nonlocal spatial interactions in two-component systems can cause

https://doi.org/10.1017/prm.2024.24 Published online by Cambridge University Press

higher codimension bifurcations and patterns, when considering the secondary bifurcation of double-Hopf bifurcations, e.g. spatially nonhomogeneous or quasi-periodic solutions. Britton [**3**] argued that if mobile animals compete for a common resource, considering the depletion of resources, intraspecific competition effects should depend on average population density in the neighbourhood of the current location, which implies that nonlocal intraspecific interactions may be more reasonable, and indeed nonlocal competitions can facilitate the coexistence of two competitors. It turns out that the nonlocal interaction can induce rich and interesting dynamics, which has attracted substantial attention in the past decade [**6**, **7**, **22**, **33**, **34**, **36**, **37**].

We would like to mention that there are different methods to model nonlocality. The first approach is to describe nonlocal diffusion by convolution integrals, we refer to the monograph by Andreu-Vaillo *et al.* [**1**] for fundamental theories of such nonlocal equations and a survey by Bates [**2**] for applications in materials science. The second approach is to use spatial integrals to characterize nonlocal effects, which has been employed in modelling population dynamics by Britton [**3**] and Gourley [**14**]. We also refer to a review by Ruan [**29**] on such nonlocal epidemiological models. In this paper, we follow the second approach, that is, we use a spatial integral to describe the nonlocal intraspecific competition among the prey population. Based on system (1.1) and [**13**], we propose the following host–parasitoid model with generalist predation:

$$\begin{cases} \dfrac{\partial u}{\partial t} = d_1 \Delta u + r_1 u\left(1 - \dfrac{1}{K_1}\displaystyle\int_\Omega G(x,y)u(y,t)\,\mathrm{d}y\right) - \dfrac{Euv}{1+Ehu},\ x \in \Omega,\ t > 0, \\ \dfrac{\partial v}{\partial t} = d_2 \Delta v + r_2 v\left(1 - \dfrac{v}{K_2}\right) + \dfrac{\gamma Euv}{1+Ehu},\ x \in \Omega,\ t > 0, \\ \dfrac{\partial u}{\partial \nu} = \dfrac{\partial v}{\partial \nu} = 0,\ x \in \partial\Omega,\ t > 0, \\ u(x,0) = u_0(x) \geqslant 0,\ v(x,0) = v_0(x) \geqslant 0,\ x \in \Omega. \end{cases} \tag{1.2}$$

The domain Ω is a region in the Euclidean space $\mathbb{R}^n$ with smooth boundary $\partial\Omega$, where ν is the outward unit vector of the boundary $\partial\Omega$, is bounded in $\mathbb{R}^n$. For the rest of this paper, we consider system (1.2) in $\Omega = (0,\, l\pi)$, $l \in \mathbb{R}^+$. The boundary conditions are homogenous Neumann boundary conditions, which means the model is self-contained with zero population flux across the boundary. The constants d_1 and d_2 denote diffusion coefficients of prey and predators, respectively. The integral term in the first equation of (1.2) accounts for the nonlocal intraspecies interactions among the prey individuals, i.e. the self-regulation of the prey species depends upon its own spatial average, weighted properly according to the spatial scale. To be more precisely, $G(x,\, y)$ can be regarded a measurement of the competition pressure at location x from the individuals at another location y. In this paper, we will analyse the following two situations in turn:

(1) Dirac kernel: $G(x,\, y) = \delta(x - y)$,

(2) Spatial average kernel: $G(x,\, y) = 1/|\Omega|$, where $|\Omega|$ denotes the volume of the habitat Ω.

https://doi.org/10.1017/prm.2024.24 Published online by Cambridge University Press

Case (1) is referred to as the local interaction, where $\delta(x)$ is the Dirac measure, which implies that the nonlocal term $\int_\Omega G(x, y)u(y, t)\,\mathrm{d}y$ in (1.2) is reduced to $u(x, t)$; while in case (2), the competition strength among all prey individuals is the same across the habitat, and we call such nonlocal interaction as the global competition, i.e. the competition between any two prey individuals is the same.

To simplify our analysis and calculations, we make the following scaling:

$$u = K_1\bar{u}, \quad v = K_2\bar{v}, \quad t = \frac{\tau}{r_1},$$

then system (1.2) becomes (still denote τ by t and drop the bar):

$$\begin{cases} \dfrac{\partial u}{\partial t} = d_1\Delta u + u(1-\hat{u}) - \dfrac{buv}{a+u}, \ x \in \Omega, \ t > 0, \\ \dfrac{\partial v}{\partial t} = d_2\Delta v + cv\left(1 - v + \dfrac{eu}{a+u}\right), \ x \in \Omega, \ t > 0, \\ \dfrac{\partial u}{\partial \nu} = \dfrac{\partial v}{\partial \nu} = 0, \ x \in \partial\Omega, \ t > 0, \\ u(x,0) = u_0(x) \geqslant 0, \ v(x,0) = v_0(x) \geqslant 0, \ x \in \Omega, \end{cases} \tag{1.3}$$

where

$$\hat{u} = \int_\Omega G(x,y)u(y,t)\,\mathrm{d}y, \quad a = \frac{1}{EK_1h}, \quad b = \frac{K_2}{r_1hK_1},$$
$$c = \frac{r_2}{r_1}, \quad e = \frac{\gamma}{r_2h}, \quad d_i \to \frac{d_i}{r_1}, \quad (i = 1, 2),$$

and a, b, c, e, d_1, d_2 are all positive constants.

In this paper, we first provide some preliminary analysis on Hopf bifurcation for the local model. Next, for the reaction–diffusion model with local intraspecific prey competition, we show the Turing instability of spatially homogeneous steady states (i.e. diffusion-induced instability), the existence of Hopf bifurcation, and Turing–Hopf bifurcation. We will rigorously prove the existence of two kinds of normal forms with different dynamics for Turing–Hopf bifurcation, where a pair of spatially nonhomogeneous periodic solutions is stable for (8,0)-mode Turing–Hopf bifurcation and unstable for (3,0)-mode Turing–Hopf bifurcation, which were seldom observed and proved in an applied problem. Our results indicate that the model exhibits complex pattern formations, including transient states, monostability, bistability, tristability, etc. Finally, numerical simulations are given to illustrate complex dynamics and verify our theoretical results. For the nonlocal intraspecific prey competition case, we follow the technique of Gourley [**14**] and Gourley and Ruan [**15**], that is, we assume that the spatial kernel takes some specific forms and reduce the nonlocal model into a local one. Then, we study the Hopf bifurcation, Turing bifurcation, and Turing–Hopf bifurcation. In addition, a new bifurcation called double-Hopf bifurcation is investigated. For the case with general spatial kernels, one could use spectral theory to analyse the stability and bifurcation of the model (see [**43**]), which deserves further consideration.

The remaining part of this paper is organized as follows. In § 2, we investigate the Hopf bifurcation for a ordinary differential equation (ODE) model.

https://doi.org/10.1017/prm.2024.24 Published online by Cambridge University Press

In § 3, we consider bifurcations of the reaction–diffusion system with local intraspecific prey competition, including Turing instability of spatially homogeneous steady states, Hopf bifurcation, Turing–Hopf bifurcation, and spatiotemporal patterns via Turing–Hopf bifurcation are provided in this part. In § 4, we focus on a reaction–diffusion system with nonlocal intraspecific prey competition, the criteria for the existence of Hopf bifurcation, Turing bifurcation, and Turing Hopf bifurcation are established, and a new bifurcation double-Hopf bifurcation is studied. Finally, we provide a summary and open problems in § 5.

We use $\mathbb{N}$ to denote a set of all positive integers, and $\mathbb{N}_0 := \mathbb{N} \cup 0$ in this paper.

2. Hopf bifurcation of the ODE system

In this section, we consider system (1.3) without spatial effects, i.e. the local system:

$$\begin{cases} \dfrac{\mathrm{d}u}{\mathrm{d}t} = u\left(1 - u - \dfrac{bv}{a+u}\right), \\ \dfrac{\mathrm{d}v}{\mathrm{d}t} = cv\left(1 - v + \dfrac{eu}{a+u}\right). \end{cases} \tag{2.1}$$

According to Xiang *et al.* [**38**], system (2.1) always has three boundary equilibria: hyperbolic unstable node $B_1(0,\,0)$, hyperbolic saddles $B_2(1,\,0)$, and $B_3(0,\,1)$ if $a > b$.

The positive equilibrium $(u,\,v)$ of system (2.1) satisfies

$$f(u) \triangleq u^3 + (2a-1)u^2 + (a^2 - 2a + be + b)u + a(b-a) = 0. \tag{2.2}$$

System (2.1) has a unique positive equilibrium $E_*(u_*,\,v_*)$ if $(a,\,b,\,c,\,e) \in U_1$, where $0 < u_* < 1$, $v_* = ((1-u_*)(a+u_*))/b$ and

$$U_1 \triangleq \left\{(a,b,c,e) | a > b, a \geqslant \frac{1}{2}, c > 0, e > 0\right\}. \tag{2.3}$$

The Jacobian matrix of system (2.1) at E_* is

$$J(E_*) = J_0 \triangleq \begin{pmatrix} s_1 - u_* & -\delta_1 \\ c\delta_2 & -cv_* \end{pmatrix},$$

where

$$s_1 = \frac{u_*(1-u_*)}{a+u_*}, \quad \delta_1 = \frac{bu_*}{a+u_*}, \quad \delta_2 = \frac{aev_*}{(a+u_*)^2}. \tag{2.4}$$

Then, we have

$$\begin{aligned} \mathrm{Det}(J_0) = \mathcal{M}_0 &\triangleq c(\delta_1\delta_2 - (s_1 - u_*)v_*) = cu_*v_*\left(1 + \frac{abe}{(a+u_*)^3} - \frac{bv_*}{(a+u_*)^2}\right), \\ \mathrm{Tr}(J_0) = \mathcal{T}_0 &\triangleq (s_1 - u_*) - cv_* = \frac{1}{a+u_*}\left[(1-a-2u_*)u_* - c(a + (1+e)u_*)\right]. \end{aligned} \tag{2.5}$$

https://doi.org/10.1017/prm.2024.24 Published online by Cambridge University Press

A simple calculation shows that

$$\mathrm{Det}(J_0) = \mathcal{M}_0 = \frac{cs_1}{b} f'(u_*) > 0. \tag{2.6}$$

Let

$$c_0^H \triangleq \frac{s_1 - u_*}{v_*} = \frac{u_*(1-a-2u_*)}{a+(1+e)u_*}, \tag{2.7}$$

we have the following results.

LEMMA 2.1. *If $(a, b, c, e) \in U_1$, then system (2.1) has a unique positive equilibrium E_*, which is unstable for $\mathrm{Tr}(J_0) > 0$, and locally asymptotically stable for $\mathrm{Tr}(J_0) < 0$. More precisely:*

(I) *if $u_* \geqslant (1-a)/2$, then E_* is locally asymptotically stable;*

(II) *if $u_* < (1-a)/2$ and*

(i) *$0 < c < c_0^H$, then E_* is unstable;*

(ii) *$c = c_0^H$, then E_* is a centre-type equilibrium;*

(iii) *$c > c_0^H$, then E_* is locally asymptotically stable.*

We next consider case (II)(ii) in lemma 2.1, and explore the existence of Hopf bifurcation at E_*. Using the formula in Perko [**28**], we obtain the first Lyapunov coefficient:

$$\sigma_1 = \frac{u_*(1-a-2u_*)\sigma_{11}}{8(a+u_*)^6(1-u_*)\mathcal{M}_0}, \tag{2.8}$$

where $\mathcal{M}_0$ is given in (2.5) and

$$\sigma_{11} = (2a^2 + a(1+3u_*)u_* + (1-3u_*+4u_*^2)u_*)ab - 2(a+u_*)^2(a^2-u_*^3)(1-u_*).$$

THEOREM 2.2. *If $(a, b, c, e) \in U_1$, $u_* < (1-a)/2$ and $a < 1$, then system (2.1) undergoes a Hopf bifurcation at E_* for $c = c_0^H$. Moreover,*

(i) *if $\sigma_{11} < 0$, then the Hopf bifurcation is supercritical and the bifurcating periodic orbit is stable;*

(ii) *if $\sigma_{11} > 0$, then the Hopf bifurcation is subcritical the bifurcating periodic orbit is unstable.*

EXAMPLE 2.3. In order to verify the conclusions of theorem 2.2, we fix $a = \frac{1}{2}$, $b = \frac{1}{4}$, and $e = \frac{95}{16}$. Select c as bifurcation parameter, then system (2.1) can be written as

$$\begin{cases} \dfrac{\mathrm{d}u}{\mathrm{d}t} = u\left(1 - u - \dfrac{v}{2+4u}\right), \\ \dfrac{\mathrm{d}v}{\mathrm{d}t} = cv\left(1 + \dfrac{95u}{8+16u} - v\right), \\ u(0) = 0.2,\ v(0) = 1.5. \end{cases} \tag{2.9}$$

https://doi.org/10.1017/prm.2024.24 Published online by Cambridge University Press

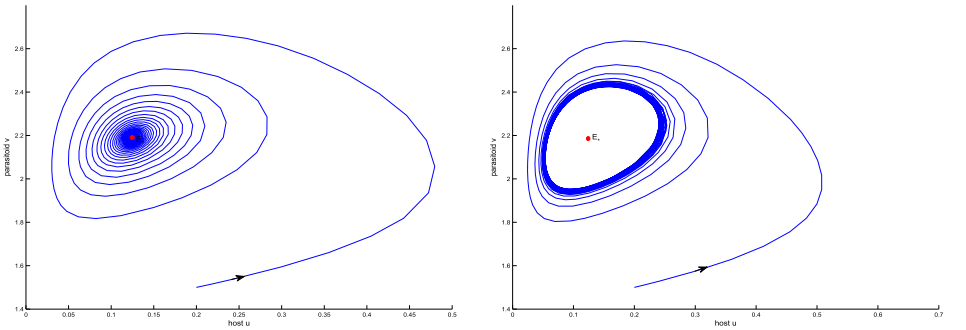

(a) (b)

Figure 1. (a) E_* of system (2.1) is stable when $c = \frac{1}{40} > c_0^H = \frac{4}{175}$; (b) E_* of system (2.1) is unstable and surrounded by a stable limit cycle when $c = \frac{1}{50} < c_0^H$.

It is easy to check that E_* is stable when $c = \frac{1}{40} > c_0^H = \frac{4}{175}$ (figure 1(a)), and a stable limit cycle, bifurcating from supercritical Hopf bifurcation at E_*, occurs when $c = \frac{1}{50} < c_0^H$ (figure 1(b)).

3. System (1.3) with local intraspecific prey competition

In this section, we consider system (1.3) with local intraspecific prey competition, i.e. the nonlocal term $\hat{u}$ in (1.3) is reduced to $u(x, t)$.

3.1. Turing instability of the reaction–diffusion system

In this subsection, we consider the Turing instability of the positive constant steady state E_* in reaction–diffusion system (1.3) when $(a, b, c, e) \in U_1$.

Proposition 3.1. *The solutions of* (1.3) *are non-negative. Moreover, the non-negative solution* (u, v) *of system* (1.3) *satisfies*

$$\limsup_{t\to\infty} \max_{\bar{\Omega}} u(x,t) \leqslant 1, \quad \limsup_{t\to\infty} \max_{\bar{\Omega}} v(x,t) \leqslant 1 + \frac{e}{1+a}.$$

Proof. Since both the u-axis and v-axis are invariant lines, if the initial values are non-negative, then solutions of system (1.3) are also non-negative. According to comparison principle, we have

$$u(1-u) - \frac{buv}{a+u} \leqslant u(1-u), \quad (x,t) \in \Omega \times [0,\infty),$$

hence, there exists a $T \in (0, \infty)$ such that $u(x, t) \leqslant 1 + \epsilon$ in $\bar{\Omega} \times [T, \infty)$ for any $\epsilon > 0$. Moreover,

$$cv\left(1 + \frac{eu}{a+u} - v\right) \leqslant cv\left(1 + \frac{e(1+\epsilon)}{a+1+\epsilon} - v\right), \quad x \in \bar{\Omega}, \quad t \in [T,\infty),$$

https://doi.org/10.1017/prm.2024.24 Published online by Cambridge University Press

then again by comparison principle, we have

$$\limsup_{t\to\infty}\max_{\bar{\Omega}} v(x,t) \leqslant 1+\frac{e+\epsilon}{1+a+\epsilon},$$

by the arbitrariness of ϵ, the conclusion holds. □

The linear part of system (1.3) is

$$\begin{pmatrix} \dfrac{\partial u}{\partial t} \\ \dfrac{\partial u}{\partial t} \end{pmatrix} = L\begin{pmatrix} u \\ v \end{pmatrix} = D\begin{pmatrix} u_{xx} \\ v_{xx} \end{pmatrix} + J\begin{pmatrix} u \\ v \end{pmatrix} \tag{3.1}$$

where

$$D = \begin{pmatrix} d_1 & 0 \\ 0 & d_2 \end{pmatrix},$$

and $J = J_0$. L is a linear operator with domain $D_L = X_C := X \oplus \mathrm{i}X = \{x_1 + \mathrm{i}x_2 : x_1,\, x_2 \in X\}$ and

$$\begin{aligned} X := \{(u,v) \in H^2[(0,l\pi)] \times H^2[(0,l\pi)] \big| u_x(0,t) = u_x(l\pi,t) \\ = v_x(0,t) = v_x(l\pi,t) = 0\}, \end{aligned}$$

where $H^2[(0,\, l\pi)]$ represent a standard Sobolev space.

Define ($k \in \mathbb{N}$):

$$J_k = \begin{pmatrix} s_1 - u_* - d_1\left(\dfrac{k}{l}\right)^2 & -\delta_1 \\ c\delta_2 & -cv_* - d_2\left(\dfrac{k}{l}\right)^2 \end{pmatrix},$$

then the corresponding characteristic equation of J_k is

$$\mathcal{P}_k(\lambda) = \lambda^2 - \mathcal{T}_k\lambda + \mathcal{M}_k, \tag{3.2}$$

in which

$$\begin{aligned} \mathcal{T}_k &= \mathcal{T}_0 - (d_1+d_2)\left(\frac{k}{l}\right)^2, \\ \mathcal{M}_k &= d_1d_2\left(\frac{k}{l}\right)^4 + (cv_*d_1 - (s_1-u_*)d_2)\left(\frac{k}{l}\right)^2 + \mathcal{M}_0. \end{aligned}$$

Obviously, B_i ($i = 1,\, 2,\, 3$) and E_* are all constant steady states. When (a, b, c, e) $\in U_1$, B_i ($i = 1,\, 2,\, 3$) are still unstable, and $E_*(u_*,\, v_*)$ is locally asymptotically stable for system (1.3) if and only if one of the following conditions holds:

(i) $u_* \geqslant (1-a)/2$;

(ii) $u_* < (1-a)/2$, $c > c_0^H$, $cv_*d_1 - (s_1-u_*)d_2 \geqslant 0$.

https://doi.org/10.1017/prm.2024.24 Published online by Cambridge University Press

Next, we study the instability and stability of the positive constant steady state E_* induced by diffusion.

Because $\mathcal{T}_k < 0$ and $\mathcal{M}_k > 0$ for any $k \geqslant 0$ when $u_* \geqslant (1-a)/2$ and $(a,\, b,\, c,\, e) \in U_1$, we consider Turing instability under the following conditions:

$$c > c_0^H, \quad u_* < \frac{1-a}{2}, \quad (a,b,c,e) \in U_1, \tag{3.3}$$

where U_1 and c_0^H are given in (2.3) and (2.7), respectively. Note that $\mathcal{T}_k < 0$ for any positive integer k if $u_* < (1-a)/2$ and $c > c_0^H$, thus to make sure Turing instability occurs, we need find the parameter conditions for $\mathcal{M}_k < 0$. Define:

$$U_2 = \left\{(a,b,c,e,u_*)|u_* < \frac{1-a}{2},\ 1 > a \geqslant \frac{1}{2},\ a > b > 0,\ c > 0,\ e > 0\right\}. \tag{3.4}$$

Next, we discuss diffusion-induced instability at E_* for system (1.3).

We define

$$\mathcal{B} = (s_1 - u_*)d_2 - cv_*d_1. \tag{3.5}$$

To ensure that Turing instability occurs, we need to find appropriate parameter conditions such that $\mathcal{M}_k < 0$ for some $k \in \mathbb{N}$. Hence, we let:

$$\mathcal{B} > 0 \quad \text{and} \quad (\mathcal{M}_k)_{\min} = \mathcal{M}_{l\sqrt{\mathcal{B}/2d_1d_2}} = \mathcal{M}_0 - \frac{\mathcal{B}^2}{4d_1d_2} < 0,$$

which are equivalent to

$$\mathcal{B} > 2\sqrt{d_1d_2\mathcal{M}_0},$$

then we have the following results.

LEMMA 3.2. *Suppose* $(a,\, b,\, c,\, e,\, u_*) \in U_2$, $c > c_0^H$ *and* $\mathcal{B} > 2\sqrt{d_1d_2\mathcal{M}_0}$, *then diffusion-induced Turing instability occurs for system* (1.3).

EXAMPLE 3.3. Choosing $(a,\, b,\, c,\, e,\, d_1,\, d_2) = (\frac{1}{2},\, \frac{1}{3},\, \frac{1}{25},\, \frac{203}{48},\, \frac{1}{18},\, 3)$, we can get $(u_*,\, v_*) = (\frac{1}{12},\, \frac{77}{48})$, and

(i) if $l = 1$, then for any positive integer k, we have $\mathcal{M}_k > 0$. Hence, E_* is a stable constant steady state with respect to systems (1.3) (see figure 2(a));

(ii) if $l = 3$, then there exists a unique positive integer $k = 2$, such that $\mathcal{M}_2 = -\frac{5921}{453\,600} < 0$. Hence, E_* is an unstable equilibrium with respect to system (1.3) (see figure 2(b)).

3.2. Bifurcations of the reaction–diffusion system

In this subsection, we discuss the Hopf bifurcation and Turing–Hopf bifurcation for system (1.3) around E_* under the parameter condition U_2, where U_2 is given in (3.4).

https://doi.org/10.1017/prm.2024.24 Published online by Cambridge University Press

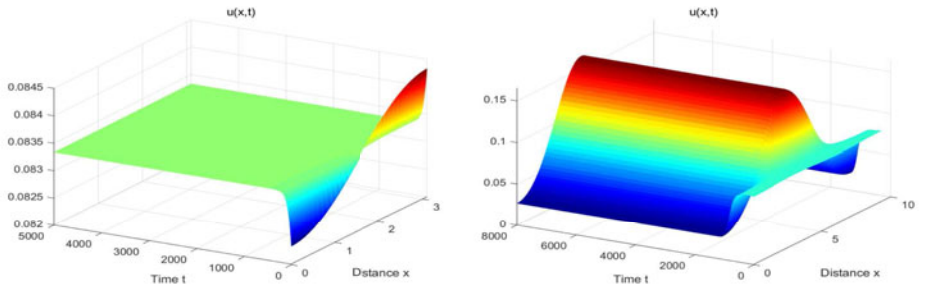

(a) (b)

Figure 2. Turing instability of the spatially homogeneous steady state $E_*(u_*, v_*)$: (a) $l = 1$, E_* is stable with respect to systems (1.3); (b) $l = 3$, E_* is unstable with respect to system (1.3). $u_0(x) = \frac{1}{12} - 0.001\cos(x)$, $v_0(x) = \frac{77}{48} + 0.001\cos(x)$.

3.2.1. Hopf bifurcation. In theorem 2.2 we discussed the existence of temporal periodic solutions for system (1.3) when all the diffusion coefficients are equal to zero. Now, we want to explore the Hopf bifurcation when the diffusion coefficients are not all zero and $(a, b, c, e, u_*) \in U_2$, where U_2 is given in (3.4).

Here, we still use c as the bifurcation parameter, the necessary conditions for a Hopf bifurcation at $c = c_i^H$ $(i = 0, 1, 2, \ldots)$ are

$$\mathcal{T}_i|_{c=c_i^H} = 0, \quad \mathcal{M}_i|_{c=c_i^H} > 0, \tag{3.6}$$

$$\mathcal{T}_j|_{c=c_i^H} \neq 0, \quad \mathcal{M}_j|_{c=c_i^H} \neq 0, \quad j \neq i, \tag{3.7}$$

where $\mathcal{T}_k$ and $\mathcal{M}_k$ are given in (3.2).

Next, we first explore the existence and bifurcating direction of spatially homogeneous periodic orbits for system (1.3), i.e. $i = 0$, $c = c_0^H$ in (3.6) and (3.7). Obviously, $\mathcal{T}_0 = 0$ and $\mathcal{M}_0 > 0$ hold for $c = c_0^H$ and $(a, b, c, e, u_*) \in U_2$. Moreover, at $c = c_0^H$, $\mathcal{T}_k < 0$ for any positive integer k. According to the expression of $\mathcal{M}_k$, we let:

$$2\sqrt{d_1 d_2 \mathcal{M}_0} > \mathcal{B}, \tag{3.8}$$

which implies that

$$(\mathcal{M}_k)_{\min} > 0 \tag{3.9}$$

for any positive integer k. Under these conditions, we have a single pair of complex eigenvalues with zero real part given by $\lambda = \pm\beta_0 \mathrm{i}$ (where $\beta_0 = \sqrt{\mathcal{M}_0}$) and

$$\left.\frac{\mathrm{dRe}(\lambda(c))}{\mathrm{d}c}\right|_{c=c^H} = -\frac{v_*}{2} \neq 0. \tag{3.10}$$

To get the stability of the bifurcated periodic solutions we need to know the behaviour of system (1.3) in its centre manifold at the bifurcation point. First, we

https://doi.org/10.1017/prm.2024.24 Published online by Cambridge University Press

define a conjugate operator of L which was defined in (3.1) as follows:

$$L^*\begin{pmatrix} u \\ v \end{pmatrix} = D\begin{pmatrix} u_{xx} \\ v_{xx} \end{pmatrix} + J^*\begin{pmatrix} u \\ v \end{pmatrix}. \tag{3.11}$$

Here, $J^* = J^T(E_*)$ and L^* are also defined in domain X.

Let:

$$q = \begin{pmatrix} q_1 \\ q_2 \end{pmatrix} = \begin{pmatrix} 1 \\ \dfrac{s_1 - u_*}{\delta_1} - \dfrac{\beta_0}{\delta_1}\mathrm{i} \end{pmatrix}, \quad q^* = \begin{pmatrix} q_1^* \\ q_2^* \end{pmatrix} = \frac{1}{2l\beta_0\pi}\begin{pmatrix} \beta_0 + (s_1 - u_*)\mathrm{i} \\ -\delta_1\mathrm{i} \end{pmatrix},$$

where $\beta_0 = \beta(c^H)$ and $\langle m, n\rangle = \int_0^{l\pi} \overline{m}^T n \,\mathrm{d}x$ for any $m \in D_{L^*}$ and $n \in D_L$, which denotes the inner product in $L^2[(0, \pi)] \times L^2[(0, \pi)]$. It is easy to check that $\langle L^*m, n\rangle = \langle m, Ln\rangle$, $Lq = \mathrm{i}\beta_0 q$, $L^*q^* = -\mathrm{i}\beta_0 q^*$, $\langle q^*, q\rangle = 1$ and $\langle q^*, \bar{q}\rangle = 0$.

Following the calculating procedure in Hassard *et al.* [**18**] (see also [**42**]), we obtain:

$$\mathrm{Re}(\sigma_1(c_0^H)) = 4\frac{u_*(1 - a - 2u_*)}{8(a + u_*)^6(1 - u_*)\mathcal{M}_0}\sigma_{11},$$

where σ_{11} is given in (2.8). Then, we have the following results.

THEOREM 3.4. *If $(a, b, c, e, u_*) \in U_2$ and $2\sqrt{d_1 d_2 \mathcal{M}_0} > \mathcal{B}$, then system (1.3) undergoes a 0-mode Hopf bifurcation around E_* at $c = c_0^H$. Moreover,*

(1) *if $\sigma_{11} < 0$, then the Hopf bifurcation is supercritical and the bifurcating (spatially homogeneous) periodic solutions are asymptotically stable;*

(2) *if $\sigma_{11} > 0$, then the Hopf bifurcation is subcritical and the bifurcating (spatially homogeneous) periodic solutions are unstable.*

EXAMPLE 3.5. Fix $a = \frac{1}{2}$, $b = d_2 = \frac{1}{3}$, and $e = \frac{7}{2}$, choose $d_1 = 0.015$ and $c = 0.03 < 0.031 = c_0^H$, then we have $\mathrm{Re}(\sigma_1(c_0^H)) = -1.615 < 0$, which means that the bifurcating periodic solutions are orbitally asymptotically stable (see figure 3).

Next, we consider the spatially nonhomogeneous Hopf bifurcations for system (1.3) with $k \geqslant 1$.

Define:

$$\mathcal{A}_1 = \delta_1\delta_2 - (s_1 - u_*)v_*, \quad \mathcal{A}_2 = \sqrt{\delta_1\delta_2(\delta_1\delta_2 - (s_1 - u_*)v_*)}, \tag{3.12}$$

where $\mathcal{A}_1 > 0$ since $\mathrm{Det}(J(E_*)) > 0$.

If $d_1 + d_2 \geqslant (s_0 - u_*)l^2$, then $\mathcal{T}_k < 0$ for any positive integer k. If $d_1 + d_2 < (s_1 - u_*)l^2$, then there exists a largest positive integer $\check{k}$ such that $(d_1 + d_2)k^2 < (s_1 - u_*)l^2$ for $1 \leqslant k \leqslant \check{k}$, and $(d_1 + d_2)k^2 \geqslant (s_1 - u_*)l^2$ for $k > \check{k}$. Moreover, from $\mathcal{T}_k = 0$

https://doi.org/10.1017/prm.2024.24 Published online by Cambridge University Press

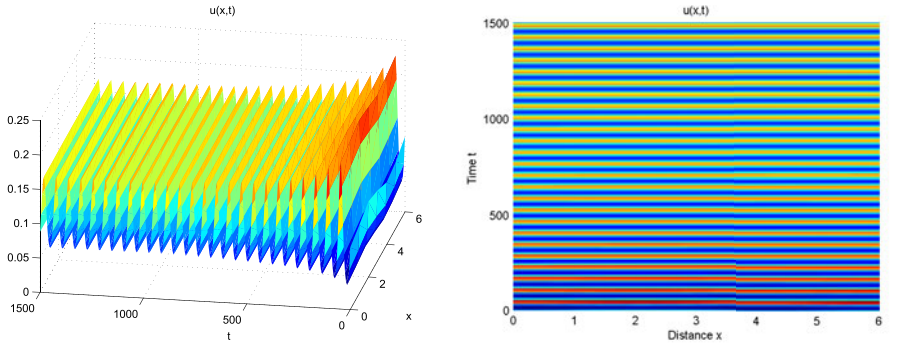

(a) (b)

Figure 3. Stable spatially homogeneous periodic solution bifurcating from 0-mode Hopf bifurcation in system (1.3), where $(a, b, e) = (\frac{1}{2}, \frac{1}{3}, \frac{7}{2})$, $l = 2$, $(d_1, d_2) = (0.015, \frac{1}{3})$, $c = 0.03 < c^H = 0.031$, $(u_0(x), v_0(x)) = (0.1 - 0.01\cos(1.5x), 1.8 - 0.05\cos(1.5x))$.

$(1 \leqslant k \leqslant \check{k})$, we have $c = c_k^H$, where

$$c_k^H = \frac{(s_1 - u_*)l^2 - (d_1 + d_2)k^2}{v_* l^2} \quad (1 \leqslant k \leqslant \check{k}). \tag{3.13}$$

On the other hand, substituting c_k^H into $\mathcal{M}_k$, we have

$$\mathcal{M}_k = \left((s_1 - u_*) - d_1\left(\frac{k}{l}\right)^2\right)\left(d_1\left(\frac{k}{l}\right)^2 + \frac{\mathcal{A}_1}{v_*}\right) - d_2\left(\frac{k}{l}\right)^2 \frac{(s_1 - u_*)v_* + \mathcal{A}_1}{v_*},$$

it is obvious that $\mathcal{M}_k < 0$ for any positive integer k if $(s_1 - u_*) \leqslant d_1(1/l)^2$. If $(s_1 - u_*) > d_1(1/l)^2$, then there exists a largest positive integer $\hat{k}$ such that $(s_1 - u_*) > d_1(k/l)^2$ for $1 \leqslant k \leqslant \hat{k}$, and $(s_1 - u_*) \leqslant d_1(k/l)^2$ for $k > \hat{k}$. It is easy to see that $\check{k} \leqslant \hat{k}$. From $\mathcal{M}_k = 0$, we have $d_2 = d_2^k \triangleq ((\mathcal{A}_1 l^2 + d_1 v_* k^2)((s_1 - u_*)l^2 - d_1 k^2))/(k^2 l^2(\mathcal{A}_1 + (s_1 - u_*)v_*))$, and d_2^k is decreasing with respect to k^2. Let:

$$d_2^* = \frac{(\mathcal{A}_1 l^2 + d_1 v_* \hat{k}^2)((s_1 - u_*)l^2 - d_1 \hat{k}^2)}{\hat{k}^2 l^2(\mathcal{A}_1 + (s_1 - u_*)v_*)}, \tag{3.14}$$

where c_0 and $\mathcal{A}_1$ are given in (2.4) and (3.12), respectively. We have the following results.

THEOREM 3.6. *Assume* $(a, b, c, e, u_*) \in U_2$, $d_1 + d_2 < (s_1 - u_*)l^2$ *and* $d_2 < d_2^*$ *hold, then system* (1.3) *undergoes a k-mode Hopf bifurcation at* $c = c_k^H$ *for* $k \in [1, \check{k}]$, *where the characteristic equation* $\mathcal{P}_k(\lambda) = 0$ *has a pair of purely imaginary roots and other roots of* $P_k(\lambda) = 0$ *with non-zero real parts.*

Proof. By $(a, b, c, e, u_*) \in U_2$, we have $(s_1 - u_*) > 0$. For fixed $k \in [1, \check{k}]$ and $c = c_k^H$, we have $\mathcal{T}_k = 0$ and $\mathcal{M}_k > 0$ since $d_1 + d_2 < (s_1 - u_*)l^2$ and $d_2 < d_2^*$. Moreover, for other integer $k \geqslant 0$, we have $\mathcal{T}_k \neq 0$ and $\mathcal{M}_k \neq 0$. These complete the proof. □

https://doi.org/10.1017/prm.2024.24 Published online by Cambridge University Press

EXAMPLE 3.7. Fixed $a = \frac{1}{2}$, $b = \frac{1}{4}$, and $e = \frac{95}{16}$, if we chose $d_1 = \frac{1}{4}$, $d_2 = \frac{1}{28}$, and $l = 8$, then $\hat{k} = \check{k} = 3$ and $d_2^* = \frac{4807}{46\,080} > \frac{1}{28}$. Hence, according to theorem 3.6, system (1.3) exhibits a k-mode Hopf bifurcation for $k = 1, 2, 3$, which are spatially nonhomogeneous.

3.2.2. Turing–Hopf bifurcation. In this subsection, we consider the existence of Turing–Hopf bifurcations around E_* in system (1.3) under the condition U_2, where U_2 is given in (3.4).

According to Jiang *et al.* [**19**], if there exists a positive integer k_1 and a non-negative integer k_2 $(k_2 \neq k_1)$ such that $\mathcal{P}_{k_1}(\lambda) = 0$ has a simple zero root and $\mathcal{P}_{k_2}(\lambda) = 0$ has a pair of purely imaginary roots, while all other eigenvalues of $\mathcal{P}_k(\lambda) = 0$ have non-zero real parts, and the corresponding transversal conditions hold, then we say that a (k_1, k_2)-mode Turing–Hopf bifurcation occurs.

Let $\mathcal{P}_k(0) = 0$ $(k \in \mathbb{N})$, then we have

$$d_1 d_2 \left(\frac{k}{l}\right)^4 + (c v_* d_1 - (s_1 - u_*) d_2) \left(\frac{k}{l}\right)^2 + c(\delta_1 \delta_2 - (s_1 - u_*) v_*) = 0,$$

from which we have

$$c = c_k(d_1) \triangleq \frac{d_2 k^2 ((s_1 - u_*) l^2 - d_1 k^2)}{v_* d_1 k^2 l^2 + \mathcal{A}_1 l^4}, \quad d_1 \in \left(0, \frac{l^2}{k^2}(s_1 - u_*)\right), \tag{3.15}$$

where $\mathcal{A}_1$ is defined in (3.12). Thus, system (1.3) may undergo k-mode Turing bifurcation if $c = c_k(d_1)$, $d_1 \in (0, ((s_1 - u_*) l^2)/k^2)$ and $k \in \mathbb{N}$.

THEOREM 3.8. *Assume* $(a, b, c, e, u_*) \in U_2$, *if* $k \geqslant k_* = \left\lfloor l\sqrt{\mathcal{A}_1/d_2 v_*} \right\rfloor + 1$, *then system* (1.3) *undergoes a* $(k, 0)$*-mode Turing–Hopf bifurcation at* E_* *for* $(d_1, c) = (d_1^k, c_0^H)$. *Moreover, when* $(d_1, c) = (d_1^{k_0^*}, c_0^H)$, *system* (1.3) *undergoes a* $(k_0^*, 0)$*-mode Turing–Hopf bifurcation, where all other eigenvalues of* $\mathcal{P}_k(\lambda) = 0$ *have negative real parts except a simple zero eigenvalue and a pair of pure imaginary eigenvalues.*

Proof. First, we denote the curves $c = c_k(d_1)$ in the (d_1, c)-plane by L_k, i.e.:

$$L_k : c = c_k(d_1), \quad 0 < d_1 < \frac{(s_1 - u_*) l^2}{k^2}, \quad k \in \mathbb{N},$$

and denote the 0-mode Hopf bifurcation curve in the (d_1, c)-plane by H_0, i.e.:

$$H_0 : c = c_0^H,$$

where c_0^H is defined in (2.6).

Second, we explore the existence of Turing–Hopf bifurcation point. From (3.15) we have $\mathrm{d}c_k(d_1)/\mathrm{d}d_1 = -(\mathrm{d}_2 \delta_1 \delta_2 k^4/((v_* d_1 k^2 + \mathcal{A}_1 l^2)^2)) < 0$, which implies that $c_k(d_1)$ is monotonically decreases in d_1. By straightforward calculation we have $\lim_{d_1 \to 0^+} c_k(d_1) = ((s_1 - u_*) d_2 k^2)/\mathcal{A}_1 l^2 > (s_1 - u_*)/v_* = c_0^H$ if $k \geqslant k_* \triangleq \left\lfloor l\sqrt{\mathcal{A}_1/d_2 v_*} \right\rfloor + 1$ ($\lfloor \cdot \rfloor$ denotes the floor function). Combining the above results

https://doi.org/10.1017/prm.2024.24 Published online by Cambridge University Press

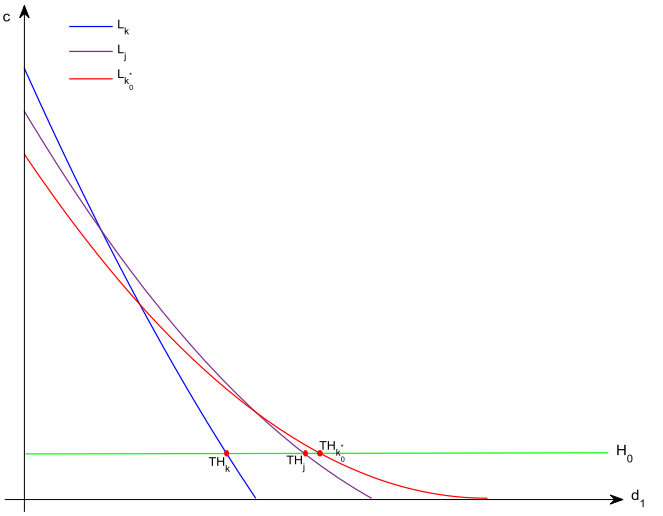

Figure 4. Turing bifurcation curves L_k, L_j, $L_{k_0^*}$, Hopf bifurcation curve H_0 and Turing–Hopf bifurcation points TH_k, TH_j, $TH_{k_0^*}$ in the (d_1, c)-plane.

with $\lim_{d_1\to((s_1-u_*)l^2)/k^2} c_k(d_1) = 0$, we know that there exists a unique $d_1 = d_1^k \in (0, (l^2(s_1-u_*))/k^2)$ such that $c_k(d_1^k) = c_0^H$ for $k \geqslant k_*$ (see figure 4). Thus, the Turing–Hopf bifurcation point $TH_k(d_1^k, c_0^H)$ exists for $k \geqslant k_*$, where

$$d_1^k = \frac{(s_1-u_*)(v_*d_2k^2 - \mathcal{A}_1l^2)l^2}{v_*k^2((s_1-u_*)l^2 + d_2k^2)}, \quad k \geqslant k_*. \tag{3.16}$$

Moreover, we have

$$\frac{\mathrm{d}d_1^k}{\mathrm{d}k^2} = \frac{(s_1-u_*)l^2(-v_*d_2^2k^4 + 2d_2\mathcal{A}_1l^2k^2 + (s_1-u_*)\mathcal{A}_1l^4)}{v_*k^4((s_1-u_*)l^2 + d_2k^2)^2}.$$

Next, we discuss the sign of $\mathrm{d}d_1^k/\mathrm{d}k^2$. It is obviously that $\mathrm{d}d_1^k/\mathrm{d}k^2$ has the same sign with $\varphi(k^2) \triangleq -v_*d_2^2k^4 + 2d_2\mathcal{A}_1l^2k^2 + (s_1-u_*)\mathcal{A}_1l^4$. Let $w = k^2$, then $\varphi(w) = -v_*d_2^2w^2 + 2d_2\mathcal{A}_1l^2w + (s_1-u_*)\mathcal{A}_1l^4$. Since $\lim_{w\to0^+}\varphi(w) = (s_1-u_*)\mathcal{A}_1l^4 > 0$, and $\lim_{w\to\infty}\varphi(w) = -\infty$, there exists a unique positive w_* satisfying $\varphi(w_*) = 0$, and $\varphi(w) > 0$ in the interval $[0, w_*)$. Denote:

$$k_m^0 \triangleq \lfloor\sqrt{w_*}\rfloor = \left\lfloor l\sqrt{\frac{\mathcal{A}_2+\mathcal{A}_1}{v_*d_2}}\right\rfloor,$$

where $\mathcal{A}_2$ is defined in (3.12). Define $k_m \triangleq \max\{k_*, k_m^0\}$, then d_1^k monotonically increases in the interval $[k_*, k_m]$ for $k_m \geqslant k_*$, and monotonically decreases in the interval $[k_m+1, \infty)$ in k.

https://doi.org/10.1017/prm.2024.24 Published online by Cambridge University Press

We denote:

$$k_0^* = \begin{cases} k_m, \text{ if } d_1^{k_m} > d_1^{k_m+1}, \\ k_m + 1, \text{ if } d_1^{k_m} < d_1^{k_m+1}, \end{cases}$$

then for any given $c = c_0^H$, $d_1^{k_0^*} = \max_{k\in\mathbb{N}}\{d_1^k\}$, which is the abscissa of Turing–Hopf bifurcation point $TH_{k_0^*}(d_1^{k_0^*}, c_0^H)$ (see figure 4). Thus, system (1.3) may undergo a $(k_0^*, 0)$-mode Turing–Hopf bifurcation, where all other eigenvalues of $\mathcal{P}_k(\lambda) = 0$ have negative real parts except a simple zero eigenvalue and a pair of pure imaginary eigenvalues. If $d_1^{k_m} = d_1^{k_m+1}$, then diffusive system (1.3) may undergo Turing–Turing–Hopf bifurcation, which is a codimension-3 bifurcation, we leave it for future consideration.

When $(d_1, c) = (d_1^{k_0^*}, c_0^H)$, we have $\mathcal{T}_0 = 0$, $\mathcal{M}_0 > 0$, $\mathcal{T}_{k_0^*} < 0$, and $\mathcal{M}_{k_0^*} = 0$. In addition, we have $\mathcal{T}_k < 0$ for any positive integer k, and $\mathcal{M}_k > 0$ for any $k \neq k_0^*$ since $d_1^{k_0^*} = \max_{k\in\mathbb{N}}\{d_1^k\}$. This implies that the real parts of the eigenvalues of $\mathcal{P}_k(\lambda) = 0$ $(k \neq 0,\ k_0^*)$ are all negative. Moreover, suppose $\lambda_1 = \alpha_1 + \mathrm{i}\beta_1$ and $\lambda_2 = \alpha_2 + \mathrm{i}\beta_2$, where $\beta_1 = \sqrt{\mathcal{M}_0}$ and $\alpha_1 = \alpha_2 = \beta_2 = 0$ when $(d_1, c) = (d_1^{k_0^*}, c_0^H)$, then we have the transversality conditions:

$$\left.\frac{\mathrm{d}\alpha_1}{\mathrm{d}c}\right|_{c=c_0^H} = -\frac{v_*}{2} < 0, \quad \left.\frac{\mathrm{d}\alpha_2}{\mathrm{d}d_1}\right|_{d_1=d_1^{k_0^*}} = \frac{(d_2\,(k/l)^2 + (s_1 - u_*))\,(k/l)^2}{T_{k_0^*}} < 0, \quad c = c_0^H. \tag{3.17}$$

The proof is completed. □

3.3. Spatiotemporal patterns via Turing–Hopf bifurcation

In this section, we calculate the normal forms of the $(k_0^*, 0)$-mode Turing–Hopf bifurcation for reaction–diffusion system (1.3) at E_*. We choose d_1 and c as bifurcation parameters, let $d_1 = d_1^{k_0^*} + \mu_1$, $c = c_0^H + \mu_2$, and obtain the unfolding system from system (1.3) as follows:

$$\begin{cases} \dfrac{\partial u}{\partial t} - (d_1^{k_0^*} + \mu_1)\Delta u = u\left(1 - u - \dfrac{bv}{a+u}\right), \ x \in (0, l\pi), \ t > 0, \\ \dfrac{\partial v}{\partial t} - d_2\Delta v = (c_0^H + \mu_2)v\left(1 - v + \dfrac{eu}{a+u}\right), \ x \in (0, l\pi), \ t > 0. \end{cases} \tag{3.18}$$

The constant steady state of system (3.18) is E_*, where u_* satisfies $f(u_*) = 0$ and $v_* = ((1-u_*)(a+u_*))/b$. To apply the generic formulas developed by Jiang *et al.* [**19**], we consider the transformation $\breve{u} = u - u_*$, $\breve{v} = v - v_*$ and drop the breves, then system (3.18) is transformed into:

$$\begin{cases} \dfrac{\partial u}{\partial t} - (d_1^{k_0^*} + \mu_1)\Delta u = (u+u_*)\left(1 - (u+u_*) - \dfrac{b(v+v_*)}{a+(u+u_*)}\right), \\ \dfrac{\partial v}{\partial t} - d_2\Delta v = (c_0^H + \mu_2)(v+v_*)\left(1 - (v+v_*) + \dfrac{e(u+u_*)}{a+(u+u_*)}\right). \end{cases} \tag{3.19}$$

According to [**19**], by a series of calculations, the normal form of system (1.3) restricted on the centre manifold up to third order at the Turing–Hopf

https://doi.org/10.1017/prm.2024.24 Published online by Cambridge University Press

singularity is

$$\begin{cases} \dot{z}_1 = a_1(\mu)z_1 + a_{200}z_1^2 + a_{011}z_2\bar{z}_2 + a_{300}z_1^3 + a_{111}z_1z_2\bar{z}_2 + h.o.t., \\ \dot{z}_2 = \mathrm{i}\omega_0 z_2 + b_2(\mu)z_2 + b_{110}z_1z_2 + b_{210}z_1^2z_2 + b_{021}z_2^2\bar{z}_2 + h.o.t., \\ \dot{\bar{z}}_2 = -\mathrm{i}\omega_0\bar{z}_2 + \bar{b}_2(\mu)\bar{z}_2 + \bar{b}_{110}z_1\bar{z}_2 + \bar{b}_{210}z_1^2\bar{z}_2 + \bar{b}_{021}z_2\bar{z}_2^2 + h.o.t., \end{cases} \tag{3.20}$$

where the coefficients can be directly calculated according to [**19**]; here, we omit the expressions for brevity. Instead, we derive concrete expressions for normal form (3.20) by fixing parameters. Then, we present bifurcation diagrams of the Turing–Hopf bifurcation and the corresponding phase portraits to exhibit spatiotemporal dynamics for diffusive system (1.3) near the Turing–Hopf singularity.

3.3.1. (3, 0)*-mode Turing–Hopf bifurcation.* In this subsection, we set $(a, b, e, d_2, l) = (\frac{1}{2}, \frac{1}{3}, \frac{7}{2}, \frac{1}{3}, 2)$. By straightforward calculations for system (1.3), we have $s_1 - u_* = 0.0505$, $\mathcal{M}_0 = 0.01169$, $(u_*, v_*) = (0.109, 1.629)$, $k_0^* = 3$, and $d_1^{k_0^*} = 0.014534$. Then, we have $k_1 = 3$ and $k_2 = 0$. The Turing bifurcation curve is

$$\begin{aligned} L_3 : c = c_3(d_1) &= \frac{\mathrm{d}_2k^2(l^2c_0 - d_1k^2)}{v_*d_1l^2k^2 + (\delta_1\delta_2 - c_0v_*)l^4} \\ &= \frac{0.0103 - 0.4604d_1}{d_1 + 0.1028}, \quad 0 < d_1 < 0.0224, \end{aligned}$$

Hopf bifurcation curve is $c = c_0^H = 0.031$, and (3, 0)-mode Turing–Hopf bifurcation point is $(d_1, c) = (0.014534, 0.031)$.

Furthermore, for the above given parameters, the normal form system (3.20) truncated to order 3 for the (3, 0)-mode Turing–Hopf bifurcation is

$$\begin{aligned} \dot{z}_1 &= -(2.3011\mu_1 + 0.5495\mu_2)z_1 - 3.2542z_1^3 - 5.9346z_1z_2\bar{z}_2, \\ \dot{z}_2 &= 0.1081iz_2 + (1.7432i - 0.8141)\mu_2z_2 + (0.01822i - 2.1171)z_1^2z_2 \\ &\quad - (1.6147 + 1.2983i)z_2^2\bar{z}_2, \\ \dot{\bar{z}}_2 &= -0.1081i\bar{z}_2 - (1.7432i + 0.8141)\mu_2\bar{z}_2 - (0.01822i + 2.1171)z_1^2\bar{z}_2 \\ &\quad - (1.6147 - 1.2983i)z_2\bar{z}_2^2. \end{aligned} \tag{3.21}$$

Let $z_1 = r$, $z_2 = \rho\cos\theta + \mathrm{i}\rho\sin\theta$, $\bar{z}_2 = \rho\cos\theta - \mathrm{i}\rho\sin\theta$, and drop the equation of θ, then system (3.21) becomes

$$\begin{aligned} \dot{r} &= -(2.3011\mu_1 + 0.5495\mu_2)r - 3.2542r^3 - 5.9346r\rho^2, \\ \dot{\rho} &= -0.8141\mu_2\rho - 2.1171r^2\rho - 1.6147\rho^3. \end{aligned} \tag{3.22}$$

https://doi.org/10.1017/prm.2024.24 Published online by Cambridge University Press

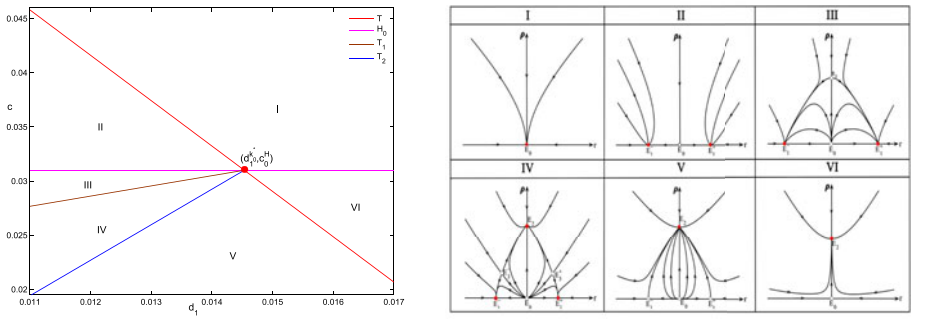

(a) (b)

Figure 5. (3, 0)-mode Turing–Hopf bifurcation diagram in the (d_1, c)-plane for system (1.3) and the corresponding phase portraits for system (3.22).

The equilibria for system (3.22) are

$$\begin{aligned}
&E_0 = (0, 0),\\
&E_1^{\pm} = (\pm\sqrt{-(0.7071\mu_1 + 0.1689\mu_2)}, 0), \quad \text{for } 0.7071\mu_1 + 0.1689\mu_2 < 0,\\
&E_2 = (0, \sqrt{-0.5042\mu_2}), \quad \text{for } \mu_2 < 0,\\
&E_3^{\pm} = (\pm\sqrt{0.5083\mu_1 - 0.5396\mu_2}, \sqrt{-0.6665\mu_1 + 0.2033\mu_2}), \quad \text{for } 0.5083\mu_1\\
&\qquad - 0.5396\mu_2 > 0, \quad -0.6665\mu_1 + 0.2033\mu_2 > 0.
\end{aligned}$$

The critical bifurcation curves for system (3.22) are

$$\begin{aligned}
&H_0 : \ \mu_2 = 0; \quad T : \ \mu_2 = -4.1876\mu_1;\\
&T_1 : \ \mu_2 = 0.9421\mu_1, \ \ \mu_1 \leqslant 0; \quad T_2 : \ \mu_2 = 3.2786\mu_1, \ \ \mu_1 \leqslant 0,
\end{aligned} \tag{3.23}$$

the dynamics and bifurcations for system (3.22) are similar to Case Ib in section 7.5 of [**16**]. Therefore, the bifurcation curves in the (d_1, c)-plane, still denoted by H_0, T, T_1, and T_2, respectively, are shown in figure 5(a), where

$$\begin{aligned}
&H_0 : \ c = c_0^H, \quad T : \ c = c_0^H - 4.1876(d_1 - d_1^{k_0^*}),\\
&T_1 : \ c = c_0^H + 0.9421(d_1 - d_1^{k_0^*}), \quad d_1 \leqslant d_1^{k_0^*},\\
&T_2 : \ c = c_0^H + 3.2786(d_1 - d_1^{k_0^*}), \quad d_1 \leqslant d_1^{k_0^*}.
\end{aligned} \tag{3.24}$$

The small neighbourhood around the point $(d_1^{k_0^*}, c_0^H)$ in the (d_1, c)-plane is divided into six regions by these bifurcation curves. In each region, the dynamics of system (3.22) can be described by the corresponding phase portraits in figure 5(b).

The equilibria E_0, E_1, $E_2^{\pm}$, and $E_3^{\pm}$ of normal form system (3.22) corresponding to the positive constant steady state, the spatially homogeneous periodic solution, the positive non-constant steady states, and spatially nonhomogeneous periodic solutions of system (1.3) (or (3.18)), respectively. Thus, the dynamics of system

https://doi.org/10.1017/prm.2024.24 Published online by Cambridge University Press

(1.3) (or (3.18)) near the Turing–Hopf bifurcation singularity in the (d_1, c)-plane can be classified as follows:

(1) When $(d_1, c) = (0.0155, 0.032) \in$ I, system (3.18) exhibit monostability: a spatially homogeneous steady state, which is asymptotically stable in region I and unstable in other regions (see figure 6).

(2) When $(d_1, c) = (0.0135, 0.032) \in$ II, system (1.3) exhibits bistability: a pair of spatially nonhomogeneous steady states. For different initial values, system (3.18) converges to one of these two spatially nonhomogeneous steady states (see figure 7).

(3) When $(d_1, c) = (0.01, 0.03) \in$ III, an unstable spatially homogeneous periodic solution occurs, and system (3.18) still exhibits bistability: a pair of spatially nonhomogeneous steady states. Moreover, system (3.18) evolves from the transient spatially homogeneous periodic solution to one of spatially nonhomogeneous steady states (see figure 8).

(4) When $(d_1, c) = (0.0135, 0.029) \in$ IV, a pair of unstable spatially nonhomogeneous periodic solutions occur, and system (3.18) exhibits tristability: two spatially nonhomogeneous steady states and a spatially homogeneous periodic solution. For different initial values, system (3.18) evolves from the spatially homogeneous steady state to a transient spatially nonhomogeneous periodic solution, and finally to the stable spatially homogeneous periodic solution (see figure 9(a) and (b)), or finally tends to one of spatially nonhomogeneous steady states (see figure 9(c)–(f)).

(5) When $(d_1, c) = (0.014, 0.025) \in$ V, a pair of unstable spatially nonhomogeneous periodic solutions disappear and system (3.18) exhibits monostability: a spatially homogeneous periodic solution (see figure 10).

(6) When $(d_1, c) = (0.0155, 0.028) \in$ VI, a pair of unstable spatially nonhomogeneous steady states disappear and system (3.18) exhibits monostability: a spatially homogeneous periodic solution (see figure 11).

3.3.2. $(8, 0)$*-mode Turing–Hopf bifurcation.* In this subsection, we set $(a, b, e, d_2, l) = (\frac{1}{2}, \frac{1}{4}, \frac{1199}{100}, \frac{1}{2}, 6)$. By straightforward calculations for system (1.3), we have $s_1 - u_* = \frac{2}{55}$, $\mathcal{M}_0 = \frac{501}{33\,275}$, $(u_*, v_*) = (\frac{1}{20}, \frac{209}{100})$, $k_0^* = 8$ and $d_1^{k_0^*} = \frac{46\,539}{4\,433\,440}$. Then, we have $k_1 = 8$ and $k_2 = 0$. The Turing bifurcation curve in the (d_1, c)-plane is

$$\begin{aligned} L_8 : c = c_8(d_1) &= \frac{\mathrm{d}_2 k^2 (l^2 c_0 - d_1 k^2)}{v_* d_1 l^2 k^2 + (\delta_1 \delta_2 - c_0 v_*) l^4} \\ &= \frac{3200(9 - 440 d_1)}{171(4509 + 19\,360 d_1)}, \quad 0 < d_1 < \frac{9}{440}. \end{aligned}$$

The Hopf bifurcation curve is $c = c_0^H = \frac{40}{2299}$, and the $(8, 0)$-mode Turing–Hopf bifurcation point is $(d_1, c) = (\frac{46\,539}{4\,433\,440}, \frac{40}{2299})$.

https://doi.org/10.1017/prm.2024.24 Published online by Cambridge University Press

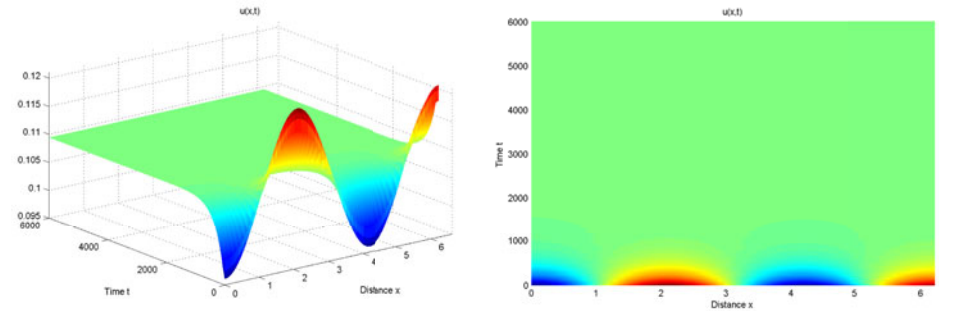

(a) (b)

Figure 6. When $(d_1, c) \in$ I in figure 5(a) for the (3, 0)-mode Turing–Hopf bifurcation, system (3.18) exhibits monostability: a positive constant steady state $E_*(0.109, 1.629)$.

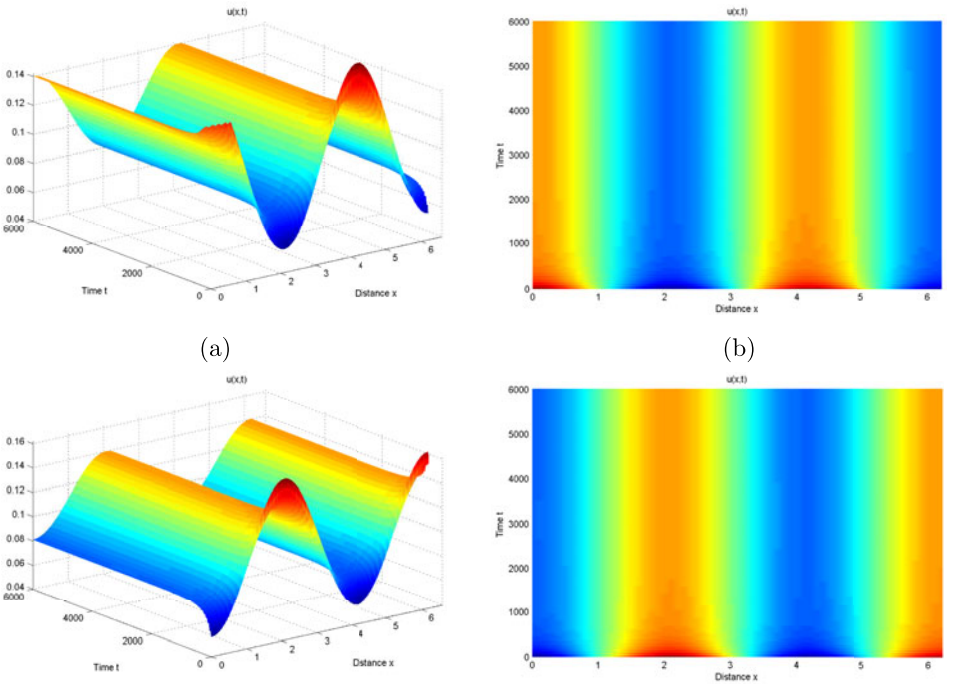

(a) (b)

(c) (d)

Figure 7. When $(d_1, c) \in$ II in figure 5(a) for the (3, 0)-mode Turing–Hopf bifurcation, system (3.18) exhibits bistability: (a),(b) One spatially nonhomogeneous steady state and (c,d): the other spatially nonhomogeneous steady state.

https://doi.org/10.1017/prm.2024.24 Published online by Cambridge University Press

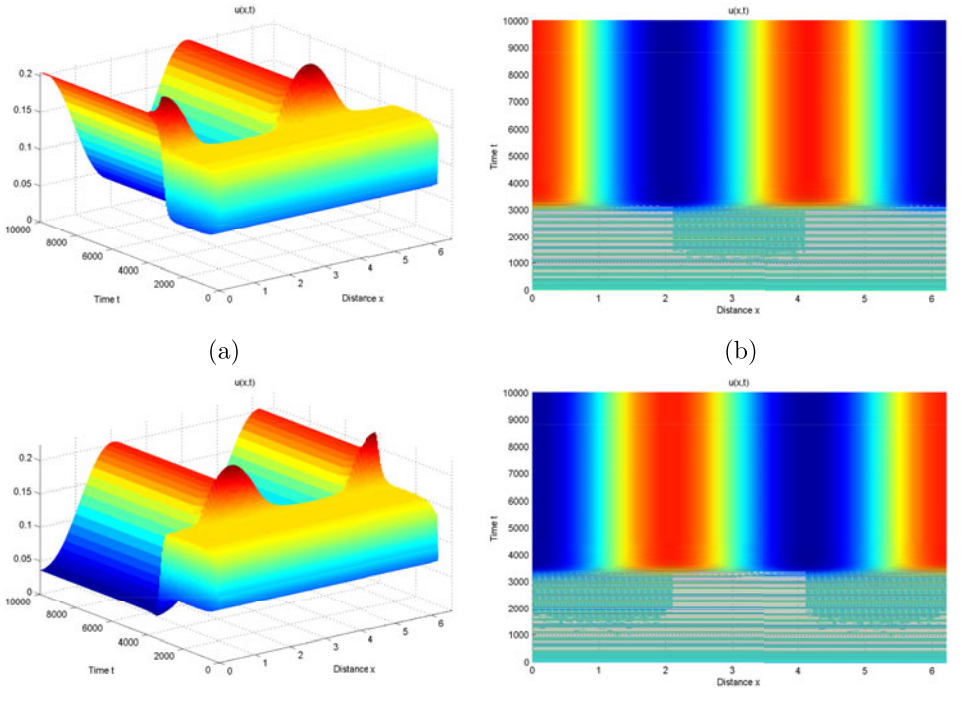

Figure 8. When $(d_1, c) \in$ III in figure 5(a) for the (3, 0)-mode Turing–Hopf bifurcation, system (3.18) exhibits an unstable spatially homogeneous periodic solution and bistability: (a, b) system (3.18) evolves from the transient spatially homogeneous periodic solution to one spatially nonhomogeneous steady stateand (c, d) to the other spatially nonhomogeneous steady state.

Furthermore, for above given parameters, the normal form system (3.20) truncated to order 3 is

$$\begin{aligned}
\dot{z}_1 &= -(1.8124\mu_1 + 0.9965\mu_2)z_1 - 5.3167z_1^3 - 5.5792z_1z_2\bar{z}_2,\\
\dot{z}_2 &= 0.1227iz_2 + (3.5262i - 1.045)\mu_2 z_2 - (2.5151i + 0.5623)z_1^2 z_2\\
&\quad - (8.1415i + 1.8222)z_2^2\bar{z}_2,\\
\dot{\bar{z}}_2 &= -0.12271i\bar{z}_2 - (3.5262i + 1.045)\mu_2\bar{z}_2 + (2.5151i - 0.5623)z_1^2\bar{z}_2\\
&\quad + (8.1415i - 1.8222)z_2\bar{z}_2^2.
\end{aligned} \tag{3.25}$$

Again let $z_1 = r$, $z_2 = \rho\cos\theta + \mathrm{i}\rho\sin\theta$, $\bar{z}_2 = \rho\cos\theta - \mathrm{i}\rho\sin\theta$, and drop the equation of θ, then system (3.25) becomes

$$\begin{aligned}
\dot{r} &= -(1.8124\mu_1 + 0.9965\mu_2)r - 5.3167r^3 - 5.5792r\rho^2,\\
\dot{\rho} &= -1.045\mu_2\rho - 0.5623r^2\rho - 1.8222\rho^3.
\end{aligned} \tag{3.26}$$

https://doi.org/10.1017/prm.2024.24 Published online by Cambridge University Press

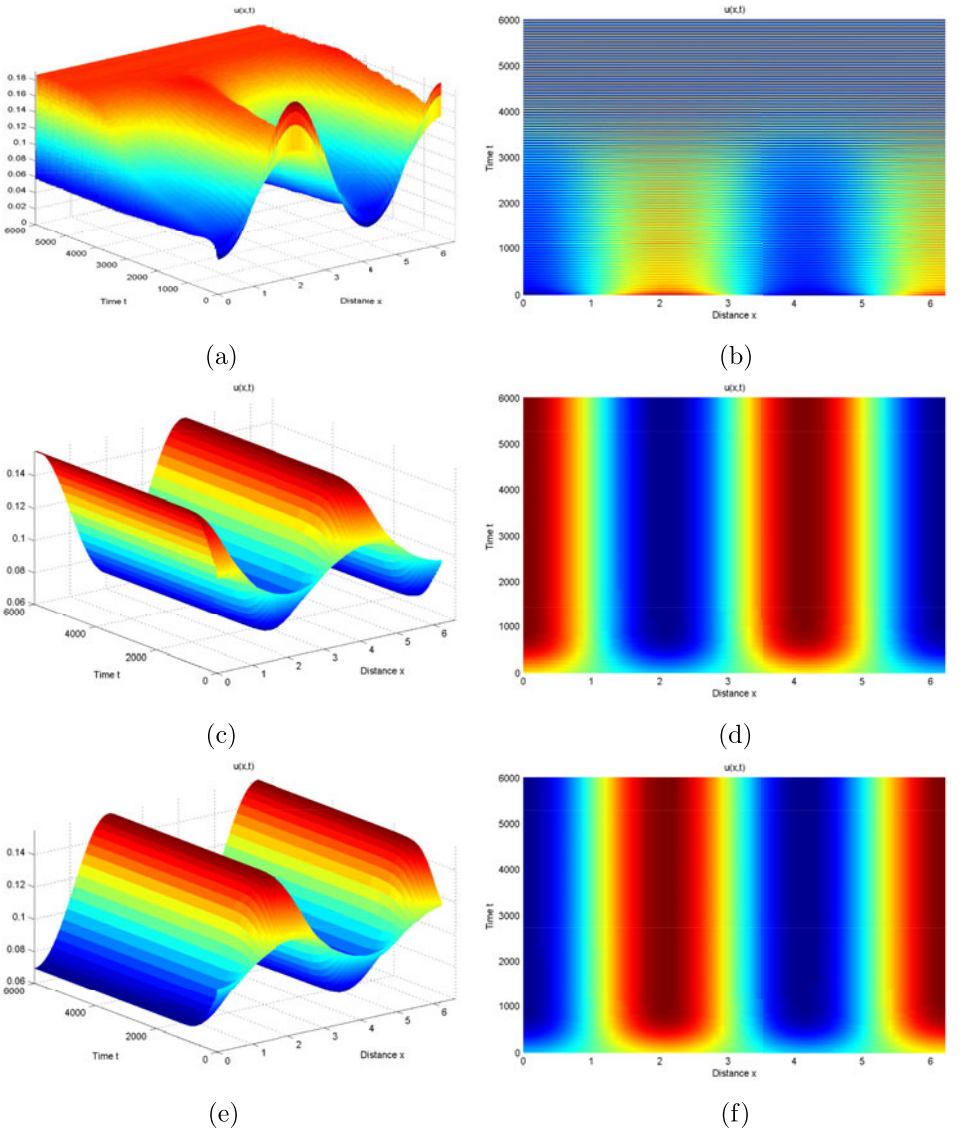

Figure 9. When $(d_1, c) \in$ IV in figure 5(a) for the (3, 0)-mode Turing–Hopf bifurcation, system (3.18) exhibits a pair of unstable spatially nonhomogeneous periodic solutions and tristability: (a, b) transient spatially nonhomogeneous periodic solutions to a stable spatially homogeneous periodic solution, (c, d) one stable spatially nonhomogeneous steady state,and (e, f) the other stable spatially nonhomogeneous steady state.

System (3.26) has equilibria

$$E_0 = (0, 0),$$

$$E_1^{\pm} = (\pm\sqrt{-(0.3409\mu_1 + 0.1874\mu_2)}, 0), \quad \text{for} \quad 0.3409\mu_1 + 0.1874\mu_2 < 0,$$

https://doi.org/10.1017/prm.2024.24 Published online by Cambridge University Press

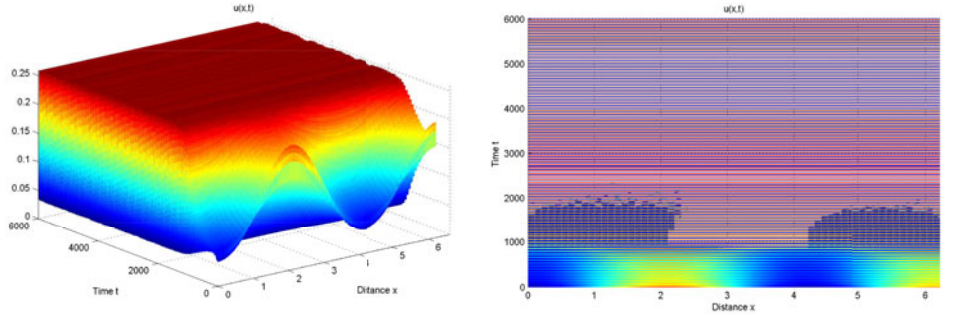

(a) (b)

Figure 10. When $(d_1, c) \in$ V in figure 5(a) for the (3, 0)-mode Turing–Hopf bifurcation, a pair of unstable spatially nonhomogeneous periodic solutions disappear and system (3.18) exhibits monostability: a spatially homogeneous periodic solution.

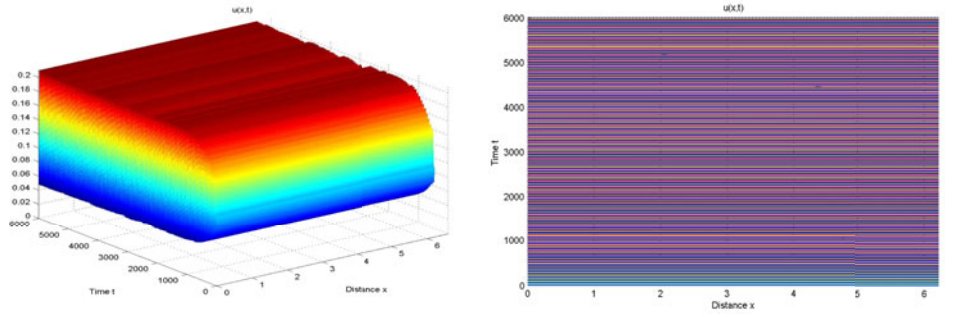

(a) (b)

Figure 11. When $(d_1, c) \in$ VI in figure 5(a) for the (3, 0)-mode Turing–Hopf bifurcation, a pair of unstable spatially nonhomogeneous steady states disappear and system (3.18) exhibits monostability: a spatially homogeneous periodic solution.

$$E_2 = (0, \sqrt{-0.5735\mu_2}), \quad \text{for} \quad \mu_2 < 0,$$
$$E_3^{\pm} = (\pm\sqrt{-0.5041\mu_1 + 0.6128\mu_2}, \sqrt{0.1556\mu_1 - 0.7626\mu_2}), \quad \text{for} \quad -0.5041\mu_1 + 0.6128\mu_2 > 0, \quad 0.1556\mu_1 - 0.7626\mu_2 > 0.$$

Similar to the (3, 0)-mode Turing–Hopf bifurcation, the critical bifurcation curves are

$$H_0: \ \mu_2 = 0; \ \ T: \ \mu_2 = -1.8177\mu_1; \ \ T_1: \ \mu_2 = 0.204\mu_1, \quad \mu_1 \leqslant 0; \ \ T_2: \ \mu_2 = 0.8227\mu_1, \ \ \mu_1 \leqslant 0. \tag{3.27}$$

The dynamics and bifurcations for system (3.26) are similar to Case Ia in section 7.5 of [**16**]. Therefore, the bifurcation curves in the (d_1, c)-plane are (still denoted

https://doi.org/10.1017/prm.2024.24 Published online by Cambridge University Press

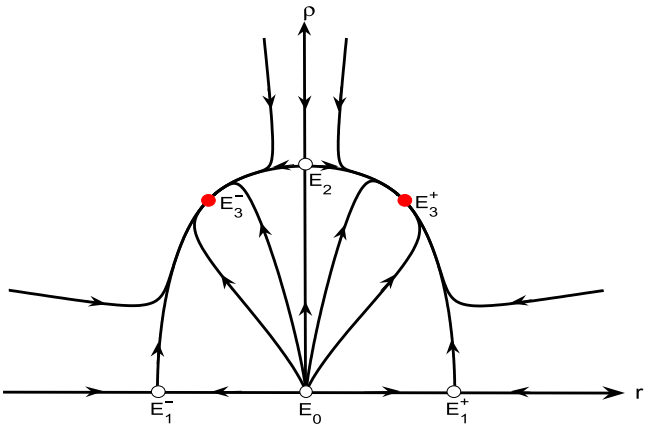

Figure 12. Phase portrait of system (3.26) for the (8, 0)-mode Turing–Hopf bifurcation when $(\mu_1, \mu_2) \in$ IV in figure 5(a).

by H_0, T, T_1, and T_2, respectively):

$$\begin{aligned} &H_0:\ c = c_0^H, \quad T:\ c = c_0^H - 1.8177(d_1 - d_1^{k_0^*}),\\ &T_1:\ \mu_2 = c_0^H + 0.204(d_1 - d_1^{k_0^*}),\ \ d_1 \leqslant d_1^{k_0^*},\\ &T_2:\ \mu_2 = c_0^H + 0.8227(d_1 - d_1^{k_0^*}),\ \ d_1 \leqslant d_1^{k_0^*}. \end{aligned} \tag{3.28}$$

Compared with the (3, 0)-mode Turing–Hopf bifurcation (similar to Case Ib in [**16**]), the (8, 0)-mode Turing–Hopf bifurcation (similar to Case Ia in [**16**]) only has some differences in region IV of figure 5, where a pair of spatially nonhomogeneous steady states and a spatially homogeneous periodic solution all turn into unstable, and a pair of spatially nonhomogeneous periodic solutions become stable (see figures 12 and 13).

4. System (1.3) with nonlocal intraspecific prey competition

In this section, we consider system (1.3) with nonlocal intraspecific prey competition, i.e. the nonlocal term $\hat{u}$ takes the following form:

$$\hat{u} := \frac{1}{l\pi}\int_0^{l\pi} u(y,t)\,\mathrm{d}y, \tag{4.1}$$

then the linearized system of (1.3) at $E_*(u_*, v_*)$ is given by

$$\begin{cases} \dfrac{\partial u}{\partial t} = d_1\Delta u - u_*\hat{u} + \dfrac{u_*(1-u_*)}{a+u_*}u - \dfrac{bu_*}{a+u_*}v,\\ \dfrac{\partial v}{\partial t} = d_2\Delta v + \dfrac{acev_*}{(a+u_*)^2}u - cv_*v,\\ u_x(0,t) = v_x(0,t) = u_x(l\pi,t) = v_x(l\pi,t) = 0, \end{cases} \tag{4.2}$$

https://doi.org/10.1017/prm.2024.24 Published online by Cambridge University Press

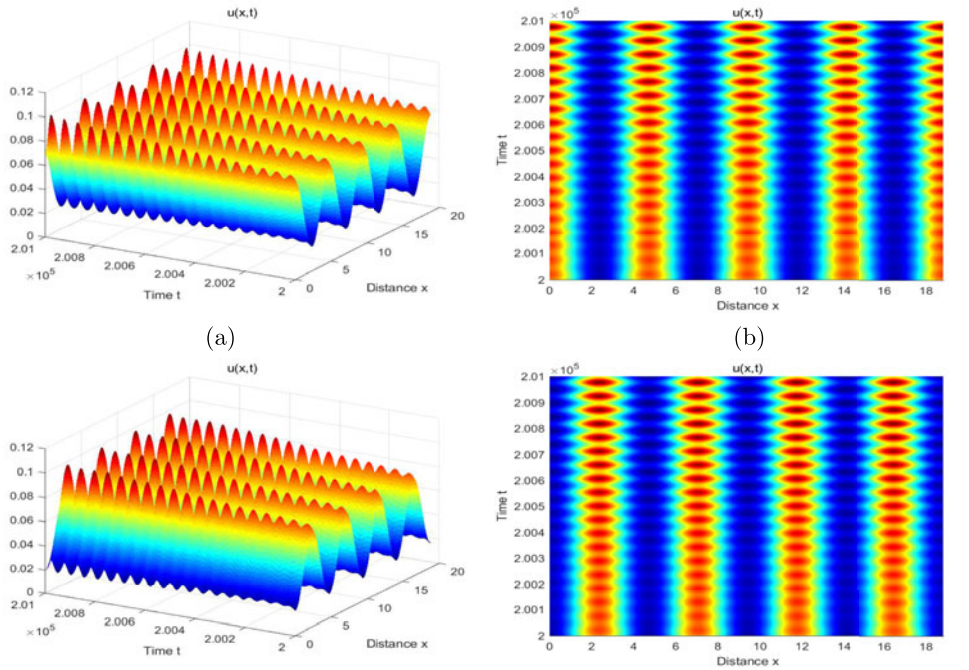

Figure 13. When $(d_1, c) \in$ IV in figure 5(a) for the (8, 0)-mode Turing–Hopf bifurcation, a spatially homogeneous steady state, a pair of spatially nonhomogeneous steady states and a spatially homogeneous periodic solution are all unstable, while a pair of spatially nonhomogeneous periodic solutions is stable: (a, b) one stable spatially nonhomogeneous periodic solution, (c, d) the other stable spatially nonhomogeneous periodic solution, where $u_0(x) = 0.05 \pm 0.03\cos(\frac{4}{3}x)$, $v_0(x) = 2.09 - 0.01\cos(\frac{4}{3}x)$, $(\mu_1, \mu_2) = (-0.001, -0.0006)$.

where $x \in (0, l\pi)$. Then, the characteristic equations of (4.2) are

$$\mathcal{P}_k(\lambda) = \lambda^2 - \mathcal{T}_k(c)\lambda + \mathcal{M}_k(c) = 0, \quad k \in \mathbb{N}_0, \tag{4.3}$$

where

$$\mathcal{T}_0 = s_1 - u_* - cv_*, \quad \mathcal{M}_0 = (s_2 - (s_1 - u_*)v_*)c, \tag{4.4}$$

and for $k \in \mathbb{N}$

$$\begin{aligned} \mathcal{T}_k(c) &= s_1 - cv_* - \frac{(d_1 + d_2)k^2}{l^2}, \\ \mathcal{M}_k(c) &= \frac{\mathrm{d}_1 d_2 k^4}{l^4} + (cv_* d_1 - s_1 d_2)\frac{k^2}{l^2} + (s_2 - s_1 v_*)c, \end{aligned} \tag{4.5}$$

where s_1 is given in (2.4) and

$$s_2 = \frac{aeu_*(1 - u_*)}{(a + u_*)^2} > 0.$$

https://doi.org/10.1017/prm.2024.24 Published online by Cambridge University Press

To guarantee the existence of Turing bifurcation, here we suppose $s_2 - s_1 v_* > 0$, i.e.:

$$u_* < \min\left\{1, \frac{(e-1)a}{1+e}\right\}, \quad e > 1. \tag{4.6}$$

Define:

$$U_3 := \left\{(a, b, e, u_*) | a \geqslant \frac{1}{2}, a > b > 0, e > 1, 0 < u_* < \min\left\{1, \frac{(e-1)a}{1+e}\right\}\right\}. \tag{4.7}$$

4.1. Hopf and double-Hopf bifurcation

In this section, we study the existence and nonexistence of Hopf bifurcation for system (1.3). Define:

$$\begin{aligned} \Gamma_1 &:= \left\{k \in \mathbb{N} | k^2 < \frac{s_1 l^2}{d_1}\right\}, \\ c_k^T &:= \frac{(s_1 - d_1 k^2/l^2) d_2 (k^2/l^2)}{s_2 - v_* s_1 + v_* d_1 (k^2/l^2)}, \quad k \in \Gamma_1. \end{aligned} \tag{4.8}$$

LEMMA 4.1. *For any $l, d_2 > 0$, $(a, b, e, u_*) \in U_3$, suppose $0 < d_1 < s_1 l^2$, then $\Gamma_1 \neq \emptyset$.*

(1) *If $k \in \mathbb{N}_0 \backslash \Gamma_1$, then $\mathcal{M}_k(c) > 0$ for any $c > 0$.*

(2) *If $k \in \Gamma_1$, then $\mathcal{M}_k(c) > 0$ for all $c > c_{k^*}^T$, where k^* is defined as follows:*

$$k^* := \begin{cases} k_0, & \text{if } c_{k_0}^T > c_{k_0+1}^T, \\ k_0 + 1, & \text{if } c_{k_0}^T < c_{k_0+1}^T, \end{cases} \tag{4.9}$$

with

$$k_0 := \left\lfloor l \sqrt{\frac{\sqrt{(s_2 - s_1 v_*) s_2} - (s_2 - s_1 v_*)}{v_* d_1}} \right\rfloor. \tag{4.10}$$

Proof. For any $l, d_2 > 0$ and $(a, b, e, u_*) \in U_3$, the assumption $0 < d_1 < s_1 l^2$ guarantees that $\Gamma_1 \neq \emptyset$. By straightforward calculation we have

$$\mathcal{M}_k(c) = \left(s_2 - s_1 v_* + v_* d_1 \frac{k^2}{l^2}\right)(c - c_k^T), \quad k \in \mathbb{N}. \tag{4.11}$$

(1) If $k = 0$, then $\mathcal{M}_0(c) > 0$ for any $c > 0$ by (2.6). For any $k \notin \Gamma_1$ and $k \in \mathbb{N}$, that is, $s_1 < d_1(k^2/l^2)$, then according to (4.8), one can get $c_k^T < 0$, then for any $c > 0$, we have $c - c_k^T > 0$, i.e. $\mathcal{M}_k(c) > 0$.

(2) In view of the expression of c_k^T in (4.8), define $\rho(\xi)$ as follows:

$$\rho(\xi) = \frac{s_1 \xi - d_1 \xi^2}{s_2 - s_1 v_* + d_1 v_* \xi}, \quad \xi > 0.$$

Through simple calculation, there exists a unique $\xi^* = (\sqrt{(s_2 - s_1 v_*) s_2} - (s_2 - s_1 v_*))/v_* d_1$, such that $\rho(\xi)$ is increasing in $(0, \xi^*)$, decreasing in (ξ^*, ∞), and

https://doi.org/10.1017/prm.2024.24 Published online by Cambridge University Press

attains the maximum at $\xi = \xi^*$. Obviously, $\xi^* < s_1/d_1$, that is, $k_0 \in \Gamma_1$, where k_0 is defined in (4.10). If $c_{k_0}^T > c_{k_0+1}^T$, then c_k^T attains the maximum in k at $k = k_0$; while if $c_k^T \leqslant c_{k+1}^T$, by $k_1 \in \Gamma_1$, we have $c_{k_0+1}^T > c_{k_0}^T$, which implies that $k_0 + 1 \in \Gamma_1$, i.e. c_k^T attains the maximum at $k = k_0 + 1$. According to the definition of k^* in (4.9), c_k^T attains the maximum in k at $k = k^*$. By (4.8) and (4.11), we know $\mathcal{M}_k(c) > 0$ if $c > c_k^T$. Hence, if $c > c_{k^*}^T$, then $\mathcal{M}_k(c) > 0$ for each $k \in \Omega_1$. □

Based upon the expression of $\mathcal{T}_0(c)$ in (4.4), the set U_3 can be divided into two disjoint regions: U_{31} and U_{32}, where

$$\begin{aligned} U_{31} :=& \left\{(a,b,e,u_*)|a \geqslant 1, a > b > 0, e > 1, 0 < u_* < \min\left\{1, \frac{(e-1)a}{1+e}\right\}\right\} \\ &\cup \left\{(a,b,e,u_*)|1 > a \geqslant \frac{1}{2}, a > b > 0, e > 1, \frac{1-a}{2} < u_* < \frac{(e-1)a}{1+e}\right\}, \\ U_{32} :=& \left\{(a,b,e,u_*)|1 > a \geqslant \frac{1}{2}, a > b > 0, e > 1, 0 < u_* < \min\left\{\frac{1-a}{2}, \frac{(e-1)a}{1+e}\right\}\right\}. \end{aligned} \tag{4.12}$$

We have the following results about the nonexistence of Hopf bifurcation.

Lemma 4.2.

(1) *For any d_1, d_2, $l > 0$, if $(a, b, e, u_*) \in U_{31}$, then $\mathcal{T}_0(c) < 0$, which implies that there is no 0-mode Hopf bifurcation of system (1.3) for any $c > 0$.*

(2) *For any d_2, $l > 0$ and $(a, b, e, u_*) \in U_3$, if $d_1 \geqslant s_1 l^2$, then for each $k \in \mathbb{N}$, $\mathcal{T}_k(c) < 0$, which implies that there is no k-mode Hopf bifurcation for any $c > 0$.*

Define:

$$\begin{aligned} c_k^H :=& \frac{s_1 - (d_1 + d_2)(k^2/l^2)}{v_*}, \\ d_{2k^*}^k :=& \frac{(s_1 - d_1(k^2/l^2))(s_2 - s_1 v_* + v_* d_1((k^*)^2/l^2))}{v_*(s_1 - d_1((k^*)^2/l^2))((k^*)^2/l^2) + (s_2 - s_1 v_* + v_* d_1((k^*)^2/l^2))(k^2/l^2)}. \end{aligned} \tag{4.13}$$

Next, we list the result about the existence of Hopf bifurcation.

Theorem 4.3. *For any $l > 0$ and $(a, b, e, u_*) \in U_{31}$, assume that $0 < d_1 < s_1 l^2$. Then, for each $k \in \Gamma_1$, if $0 < d_2 < d_{2k^*}^k$, system (1.3) undergoes a k-mode Hopf bifurcation near E_* at $c = c_k^H$, and the bifurcating periodic orbits are spatially nonhomogeneous, where $k^* \in \Omega_1$ is defined in (4.9).*

Proof. For any $l > 0$ and $(a, b, e, u_*) \in U_{31}$, the assumption $0 < d_1 < s_1 l^2$ guarantees that Γ_1 is nonempty. Let $\mathcal{T}_k(c) = 0$, then one can get $c = c_k^H$ with c_k^H defined

https://doi.org/10.1017/prm.2024.24 Published online by Cambridge University Press

in (4.13). By simple calculation

$$\begin{cases} c_k^H(d_2) > c_{k^*}^T(d_2), \text{ for } 0 < d_2 < d_{2k^*}^k, \\ c_k^H(d_2) = c_{k^*}^T(d_2), \text{ for } d_2 = d_{2k^*}^k, \\ c_k^H(d_2) < c_{k^*}^T(d_2), \text{ for } d_2 > d_{2k^*}^k, \end{cases} \tag{4.14}$$

and $d_{2k^*}^k$ is given in (4.13). Obviously, $c_k^H(d_2) > 0$ for $0 < d_2 < d_{2k^*}^k$. Hence, $c_k^H(d_2) > c_{k^*}^T(d_2)$ if $0 < d_2 < d_{2k^*}^k$. By lemma 4.1(2), we can know that $\mathcal{M}_j(c_k^H(d_2)) > 0$ for any $j \in \Omega_1$. By lemma 4.1(1), $\mathcal{M}_j(c) > 0$ for any $j \in \mathbb{N}_0 \backslash \Gamma_1$ and $c > 0$. Hence, $\mathcal{M}_j(c_k^H(d_2)) > 0$.

For each $k \in \Gamma_1$, $\mathcal{T}_k(c_k^H(d_2)) = 0$. According to lemma 4.2, $\mathcal{T}_0(c) < 0$ for all $c > 0$ as $(a, b, e, u_*) \in U_{31}$. In particular, $\mathcal{T}_0(c_k^H(d_2)) < 0$. For any $j \in \mathbb{N}$, $j \neq k$, note that $\mathcal{T}_j(c_k^H(d_2)) \neq 0$ since $\mathcal{T}_j(c)$ is decreasing in j. Therefore, $\mathcal{P}_k(\lambda) = 0$ has a pair of purely imaginary eigenvalues, all other eigenvalues have nonzero real parts. Moreover, suppose that $\lambda_1(c) = \alpha_1(c) \pm \mathrm{i}\omega_1(c)$ is a pair of roots of the characteristic equation $\mathcal{P}_k(\lambda) = 0$ near $c = c_k^H$ with $\alpha_1(c_k^H) = 0$, $\omega_1(c_k^H) > 0$, then

$$\frac{\mathrm{d}(\alpha_1(c_k^H))}{\mathrm{d}c} = -\frac{v_*}{2} < 0, \tag{4.15}$$

which implies that the transversality condition is fulfilled. The proof is complete. □

Next, we define the Hopf bifurcation curves in the (d_2, c)-plane as

$$\begin{aligned} H_0 &: \ c = c_0^H = \frac{s_1 - u_*}{v_*}, \\ H_k &: \ c = c_k^H(d_2), \ 0 < d_2 < \frac{sl^2}{k^2} - d_1, \ k \in \Gamma_1. \end{aligned} \tag{4.16}$$

THEOREM 4.4. *For any $l > 0$, $(a, b, e, u_*) \in U_{32}$ and $u_* l^2 \leqslant d_1 < s_1 l^2$, we have the following statements hold:*

(1) *If $0 < d_2 < d_{2k^*}^0$, then system (1.3) undergoes a 0-mode Hopf bifurcation near E_* at $c = c_0^H$, the bifurcating periodic orbit is spatially homogeneous, where c_0^H and k^* are defined in (4.16) and (4.9), respectively:*

$$d_{2k^*}^0 := \frac{(s_1 - u_*)(s_2 - s_1 v_* + v_* d_1((k^*)^2/l^2))}{v_*(s_1 - d_1((k^*)^2/l^2))((k^*)^2/l^2)}. \tag{4.17}$$

(2) *For each $k \in \Gamma_1$, if $0 < d_2 < d_{2k^*}^k$, then system (1.3) undergoes a k-mode Hopf bifurcation near E_* at $c = c_k^T$, and the bifurcating periodic orbit is spatially nonhomogeneous, where c_k^H and $d_{2k^*}^k$ are defined in (4.13).*

Proof. For any $l > 0$ and $(a, b, e, u_*) \in U_{32}$, then $s_1 > u_*$, hence, $c_0^H > 0$. According to (4.4), we have $\mathcal{T}_0(c_0^H) = 0$ and $\mathcal{M}_0(c_0^H) > 0$. Since $u_* l^2 \leqslant d_1 < s_1 l^2$, then Γ_1 is nonempty, and for any $k \in \Gamma_1$, H_0 is above H_k, i.e. $c_0^H > c_k^H(d_2)$ for any $d_2 > 0$.

https://doi.org/10.1017/prm.2024.24 Published online by Cambridge University Press

(1) By direct calculation we have

$$\begin{cases} c_0^H > c_{k^*}^T(d_2), & \text{for } 0 < d_2 < d_{2k^*}^0, \\ c_0^H = c_{k^*}^T(d_2), & \text{for } d_2 = d_{2k^*}^0, \\ c_0^H < c_{k^*}^T(d_2), & \text{for } d_2 > d_{2k^*}^0, \end{cases} \tag{4.18}$$

then, $c_0^H > c_{k^*}^T(d_2)$ if $0 < d_2 < d_{2k^*}^0$. By lemma 4.1(2), $\mathcal{M}_j(c_0^H) > 0$ for each $j \in \Gamma_1$. For any $j \in \mathbb{N}_0 \backslash \Gamma_1$, according to lemma 4.1(1), $\mathcal{M}_j(c) > 0$ for all $c > 0$. Hence, $\mathcal{M}_j(c_0^H) > 0$.

Obviously, $\mathcal{T}_0(c_0^H) = 0$. For each $j \in \Gamma_1$, $\mathcal{T}_j(c_j^H) = 0$ by (4.4) and (4.13). Since $\mathcal{T}_j(c)$ is decreasing in c and $c_0^H > c_k^H(d_2)$ for any $d_2 > 0$, then $\mathcal{T}_j(c_0^H) < \mathcal{T}_j(c_j^H) = 0$. Note that for each $j \in \mathbb{N} \backslash \Gamma_1$, $d_1 j^2 > s_1 l^2$, then $\mathcal{T}_j(c) < -cv_* - d_2(k^2/l^2) < 0$ for any positive c. Hence, the characteristic equation $\mathcal{P}_0(\lambda) = 0$ has a pair of purely imaginary eigenvalues, and all the other eigenvalues have nonzero real parts. Moreover, here we suppose $\lambda_1(c) = \alpha_1(c) \pm \mathrm{i}\omega_1(c)$ is a pair of roots of characteristic equation $\mathcal{P}_0(\lambda) = 0$ near $c = c_0^H$ with $\alpha_1(c_0^H) = 0$ and $\omega_1(c_0^H) > 0$. By simple calculation:

$$\frac{\mathrm{d}\alpha_1(c_0^H)}{\mathrm{d}c} = -\frac{v_*}{2} < 0, \tag{4.19}$$

thus the transversality condition holds.

(2) For each $k \in \Gamma_1$, we have $\mathcal{T}_k(c_k^H) = 0$, $\mathcal{T}_0(c_k^H) > 0$, since $c_0^H > c_k^H(d_2)$ for any $d_2 > 0$, and $\mathcal{T}_0(c)$ is decreasing in c. By lemma 4.1(1), $\mathcal{M}_0(c_k^H) > 0$, then we can prove result (2) by using a similar argument as in the proof of theorem 4.3. □

Define:

$$\Gamma_2 := \left\{ k \in \mathbb{N} | k^2 < \frac{u_* l^2}{d_1} \right\},$$
$$\bar{d}_{2k} := \frac{u_* l^2}{k^2} - d_1, \quad k \in \Gamma_2. \tag{4.20}$$

THEOREM 4.5. *For any $l > 0$ and $(a, b, e, u_*) \in U_{32}$, if $0 < d_1 < u_* l^2$, then we have the following statements hold:*

(1) *for any $k \in \Gamma_2$ and $\bar{d}_{2k} < d_{2k^*}^0$:*

   (a) *if $0 < d_2 < d_{2k^*}^0$ and $d_2 \neq \bar{d}_{2j}$ for all $j \in \Gamma_2$, then system (1.3) undergoes a 0-mode Hopf bifurcation near E_* at $c = c_0^H$, and the bifurcating periodic orbit is spatially homogeneous;*

   (b) *if $0 < d_2 < d_{2k^*}^k$ and $d_2 \neq \bar{d}_{2k}$, then system (1.3) undergoes a k-mode Hopf bifurcation near E_* at $c = c_k^H$, the bifurcating periodic orbit is spatially nonhomogeneous.*

(2) *For each $k \in \Gamma_2$ and $\bar{d}_{2k} > d_{2k^*}^0$, or $k \in \Gamma_1 \backslash \Gamma_2$, the same conclusion as in theorem 4.4 holds,*

where c_k^H, $d_{2k^*}^k$, and $d_{2k^*}^0$ are given in (4.13) and (4.17), respectively.

https://doi.org/10.1017/prm.2024.24 Published online by Cambridge University Press

Proof. For simplicity, we only prove case (1), since case (2) can be proved by the same argument as in theorem 4.3.

For any $l > 0$ and $(a, b, e, u_*) \in U_{32}$, we have $s_1 > u_*$, then $c_0^H > 0$. If $0 < d_2 < u_* l^2$, then Γ_2 is nonempty, H_0 and H_k can intersect at $d_2 = \bar{d}_{2k}$ for $k \in \Gamma_2$, which implies that $\mathcal{T}_0(\bar{d}_{2k}) = \mathcal{T}_k(\bar{d}_{2k}) = 0$ for each $j \in \Gamma_2$.

(1)(a) If $0 < d_2 < d^0_{2k^*}$, according to (4.18), $c_0^H > c_k^T(d_2)$. Then, by lemma 4.1(2), $\mathcal{M}_j(c_0^H) > 0$ holds for each $j \in \Gamma_1$. While for $j \in \mathbb{N}_0 \backslash \Gamma_1$, by lemma 4.1(1), $\mathcal{M}_j(c) > 0$ for any $c > 0$, which means, $\mathcal{M}_j(c_0^H) > 0$.

In addition, we know that $\mathcal{T}_0(c_0^H) = 0$. Since $d_2 \neq \bar{d}_{2j}$ for any $j \in \Gamma_2$, then $\mathcal{T}_j(c_0^H) \neq 0$ for each $j \in \Gamma_2$. For any $j \notin \Gamma_2$, i.e. $d_1 j^2 > u_* l^2$, then

$$\mathcal{T}_j(c_0^H) = s_1 - v_* c_0^H - (d_1 + d_2)\frac{j^2}{l^2} \leqslant s_1 - u_* - v_* c_0^H - d_2 \frac{j^2}{l^2} = -d_2 \frac{j^2}{l^2} < 0.$$

Thus, the characteristic equation $\mathcal{P}_0(\lambda) = 0$ has a pair of purely imaginary eigenvalues, and all the other eigenvalues have nonzero real parts.

(1)(b) If $0 < d_2 < d^k_{2k^*}$, by using the same methods as in the proof of theorem 4.3, one can easily check that $\mathcal{M}_j(c_i^H) > 0$ for any $j \in \mathbb{N}_0$. In addition, $\mathcal{T}_j(c_j^H) = 0$. As $d_2 \neq \bar{d}_{2k}$, then $\mathcal{T}_0(c_j^H) \neq 0$. Note that $\mathcal{T}_j$ is decreasing in j, then for any $k \in \mathbb{N}$ and $k \neq j$, $\mathcal{T}_k(c_j^H) \neq 0$. Hence, the characteristic equation $\mathcal{P}(\lambda) = 0$ has a pair of purely imaginary eigenvalues, an all other eigenvalues have nonzero real parts. Moreover, the corresponding transversality conditions are given by (4.19) and (4.15), respectively. The proof of (1) is complete. □

According to the definition of double-Hopf bifurcation, we know that system (1.3) exhibits a double-Hopf bifurcation if the corresponding linear system has two pairs of purely imaginary eigenvalues at a singular point, and all the other eigenvalues have nonzero real parts. Next, we consider the interactions among Hopf bifurcations with different spatial modes and determine when system (1.3) will exhibit double-Hopf bifurcation. By (4.13), we know that c_k^H is decreasing in k, which implies that for any distinct positive integers k and j, there is no (k, j)-mode double-Hopf bifurcation. For the existence of $(0, k)$-mode double-Hopf bifurcation we have the following result.

THEOREM 4.6. *For any $l > 0$ and $(a, b, e, u_*) \in U_{32}$, assume that $0 < d_1 < u_* l^2$ and $\bar{d}_{2k} < d^0_{2k^*}$, then for each $k \in \Gamma_2$, system (1.3) undergoes a $(0, k)$-mode double-Hopf bifurcation near E_* at $(d_2, c) = (\bar{d}_{2k}, c_0^H)$, where c_0^H, $d^0_{2k^*}$, $\bar{d}_{2k}$, and Γ_2 are defined in (4.16), (4.17) and (4.20), respectively.*

Proof. For any $l > 0$ and $(a, b, e, u_*) \in U_{32}$, we have $s_1 > u_*$, then $c_0^H > 0$. If $0 < d_1 < u_* l^2$, then Γ_1 and Γ_2 are nonempty, which means that H_0 and H_k can intersect at $(d_2, c) = (\bar{d}_{2k}, c_0^H)$ for each $k \in \Gamma_2$, i.e. $\mathcal{T}_0(c_0^H) = \mathcal{T}_k(c_0^H)$ for each $k \in \Gamma_2$. Since c_k^H is decreasing in k, then $\mathcal{T}_j(c_0^H) \neq 0$ for any positive integer j $(j \neq k)$.

If $0 < d_2 < d^0_{2k*}$, by (4.18), $c_0^H > c^T_{k^*}$, then according to lemma 4.1(2) we have $\mathcal{M}_j(c_0^H) > 0$ for any $j \in \Gamma_1$. For $j \in \mathbb{N}_0 \backslash \Gamma_1$, according to lemma 4.1(1) $\mathcal{M}_j(c) > 0$ holds for any positive c. Hence, for any $j \in \mathbb{N}_0$, $\mathcal{M}_j(c_0^H) > 0$ holds. Thus, $\mathcal{P}_0(\lambda) = 0$ and $\mathcal{P}_k(\lambda) = 0$ $(k \in \Gamma_2)$ have a pair of pure imaginary eigenvalues, and

https://doi.org/10.1017/prm.2024.24 Published online by Cambridge University Press

all other eigenvalues have nonzero real parts. Moreover, by (4.19) and (4.15) the corresponding transversality conditions are fulfilled. □

REMARK 4.7. By (3.2), we know that when system (1.3) has local intraspecific prey competition, it will not exhibit double-Hopf bifurcation, that is, the local interactions cannot induce double-Hopf bifurcation.

4.2. Turing and Turing–Hopf bifurcations

In this subsection, we consider the Turing and Turing–Hopf bifurcations, and derive the sufficient conditions for the existence of Turing–Hopf and Turing–double-Hopf bifurcations.

By lemma 4.1(1) we know that if $d_1 \geqslant s_1 l^2$, $\mathcal{M}_k(c) > 0$ for any $c > 0$, which implies that there is no Turing bifurcation of (1.3) for each $k \in \mathbb{N}$. Next, we consider the existence of Turing bifurcation.

LEMMA 4.8. *Suppose* $0 < d_1 < s_1 l^2$ *and* $c^T_{k_0} \neq c^T_{k_0+1}$, *then we have the following statements hold:*

(1) *if* $(a, b, e, u_*) \in U_{31}$, *then for* $d_2 > d^1_{2k^*}$, *system* (1.3) *undergoes a* k^**-mode Turing bifurcation near* E_* *at* $c = c^T_{k^*}$.

(2) *if* $(a, b, e, u_*) \in U_{32}$, *then for* $d_2 > \max\{d^0_{2k^*}, d^1_{2k^*}\}$, *system* (1.3) *undergoes a* k^**-mode Turing bifurcation near* E_* *at* $c = c^T_{k^*}$.

Proof. The assumption $0 < d_1 < s_1 l^2$ guarantees that Γ_1 is nonempty, and according to lemma 4.1(2), $k^* \in \Gamma_1$, and $c^T_{k^*} > 0$.

(1) If $(a, b, e, u_*) \in U_{31}$, then $\mathcal{T}_0(c) < 0$ for any $c > 0$, which implies that $\mathcal{T}_0(c^T_{k^*}) < 0$. If $d_2 > d^1_{2k^*}$, according to (4.14) we have $c^T_{k^*}(d_2) > c^H_1(d_2)$, then for each $k \in \mathbb{N}$:

$$\mathcal{T}_k(c^T_{k^*}(d_2)) \leqslant \mathcal{T}_1(c^T_{k^*}(d_2)) < \mathcal{T}_1(c^H_1(d_2)) = 0. \tag{4.21}$$

Moreover, $\mathcal{M}_k(c^T_{k^*}(d_2)) = 0$, that is the characteristic equation $\mathcal{P}_{k^*}(\lambda) = 0$ has a simple zero eigenvalue. Next, we will show that all other eigenvalues have nonzero real parts. According to (4.21) and $\mathcal{T}_0(c^T_{k^*}) < 0$, for each non-negative integer k, $\mathcal{P}_k(\lambda) = 0$ has no purely imaginary eigenvalues. If $k \notin \Gamma_1$, then by lemma 4.1(1), $\mathcal{M}_k(c) > 0$ for any $c > 0$. For $k \in \Gamma_1$ and $k \neq k^*$, according to lemma 4.1(2), $\mathcal{M}_k(c^T_{k^*}) > 0$ as $c^T_{k_0} \neq c^T_{k_0+1}$. Hence, $\mathcal{P}_k(\lambda) = 0$ has no zero real part eigenvalue for each $k \neq k^*$.

(2) If $(a, b, e, u_*) \in U_{32}$, then $c^H_0 > 0$. When $d_2 > \max\{d^0_{2k^*}, d^1_{2k^*}\}$, according to (4.14) and (4.18), we have $c^T_{k^*}(d_2) > \max\{c^H_0, c^H_1(d_2)\}$, that is $\mathcal{T}_0(c^T_{k^*}(d_2)) < 0$ and $\mathcal{T}_0(c^T_k(d_2)) < 0$ for each $k \in \mathbb{N}$. In addition, as $c^T_{k_0} \neq c^T_{k_0+1}$, by lemma 4.1, $\mathcal{M}_k(c^T_{k^*}) > 0$ for any $k \in \mathbb{N}$ and $k \neq k^*$. Then, $\mathcal{P}_{k^*}(\lambda) = 0$ has a simple zero eigenvalue and all other eigenvalues have nonzero real parts.

Moreover, suppose that $\lambda_2(c) = \alpha_2(c) + \mathrm{i}\omega_2(c)$ is a complex eigenvalue of the characteristic equation $\mathcal{P}_{k^*}(\lambda) = 0$ near $c = c^T_{k^*}$ with $\alpha_2(c^T_{k^*}) = \omega_2(c^T_{k^*}) = 0$. By

https://doi.org/10.1017/prm.2024.24 Published online by Cambridge University Press

straightforward calculation:

$$\frac{\mathrm{d}(\alpha_2(c^T_{k^*}))}{\mathrm{d}c} = \frac{s_2 - s_1 v_* + v_* d_1((k^*)^2/l^2)}{\mathcal{T}_{k^*}(c^T_{k^*})} < 0. \tag{4.22}$$

Thus, the transversality condition is fulfilled. □

REMARK 4.9. $c^T_{k_0} = c^T_{k_0+1}$ is equivalent to d_1 taking some special values, in this case system (1.3) may undergo a (k_0, k_0+1)-mode Turing–Turing bifurcation, this left for our future work.

Now, we analyse the Turing–Hopf bifurcation. By theorems 4.3–4.5 and lemma 4.8, we know that the positive constant steady state may be destabilized through a 0-mode or k-mode Hopf bifurcation (or k-mode Turing bifurcation). Next, we turn to study the $(k, 0)$-mode and $(k, 1)$-mode Turing–Hopf bifurcations.

Define:

$$\begin{aligned} &T_{k^*} : c = c^T_{k^*}(d_2), \quad d_2 > 0, \\ &c^0_{k^*} := c^H_0, \\ &c^1_{k^*} := c^H_1(d^1_{2k^*}), \end{aligned} \tag{4.23}$$

where $c^T_{k^*}$ and k^* are defined in (4.8) and (4.9), respectively.

THEOREM 4.10. *For any $l > 0$ and $(a, b, e, u_*) \in U_{31}$, assume that $0 < d_1 < s_1 l^2$, $k^* > 1$, and $c^T_{k_0} \neq c^T_{k_0+1}$, then system (1.3) undergoes a $(k^*, 1)$-mode Turing–Hopf bifurcation near E_* at $(d_2, c) = (d^1_{2k^*}, c^1_{k^*})$. Moreover, the real parts of other eigenvalues for the characteristic equation (4.3) are negative except for a pair of purely imaginary eigenvalues and a simple zero eigenvalue, where k^*, k_0, $d^1_{2k^*}$, and $c^1_{k^*}$ are given in (4.9), (4.10), (4.13), and (4.23), respectively (see figure 14(d)).*

Proof. By lemma 4.2, we know that there is no 0-mode Hopf bifurcation if $(a, b, e, u_*) \in U_{31}$. The assumption $0 < d_1 < s_1 l^2$ guarantees that Γ_1 is nonempty. Let $c^H_1(d_2) = c^T_{k^*}(d_2)$, we can obtain the intersection of H_1 and T_{k^*} is $(d^1_{2k^*}, c^1_{k^*})$.

When $(d_2, c) = (d^1_{2k^*}, c^1_{k^*})$, $\mathcal{T}_0(d^1_{2k^*}, c^1_{k^*}) < 0$ for $(a, b, e, u_*) \in U_{31}$, and $\mathcal{T}_1(d^1_{2k^*}, c^1_{k^*}) = 0$. Since $\mathcal{T}_k$ is decreasing in k, then for any $k \in \mathbb{N}$:

$$\mathcal{T}_k(d^1_{2k^*}, c^1_{k^*}) < \mathcal{T}_1(d^1_{2k^*}, c^1_{k^*}) = 0,$$

which implies that $\mathcal{T}_{k^*}(d^1_{2k^*}, c^1_{k^*}) < 0$ as $k^* > 1$. In addition, $\mathcal{M}_{k^*}(d^1_{2k^*}, c^1_{k^*}) = 0$. Thus, $\mathcal{P}_{k^*}(\lambda) = 0$ has a simple zero, and for any $k \neq 1$, $\mathcal{P}_k(\lambda) = 0$ has no purely imaginary roots.

For any $k \in \Gamma_1$ and $k \neq k^*$, we have $c^1_{k^*} = c^H_1(d^1_{2k^*}) = c^T_{k^*}(d^1_{2k^*}) > c^T_k(d^1_{2k^*})$, then according to lemma 4.1(2) and $c^T_{k_0} \neq c^T_{k_0+1}$, $\mathcal{M}_k(d^1_{2k^*}, c^1_{k^*}) > 0$ holds for each $k \in \Gamma_1$ and $k \neq k^*$. Since $k^* > 1$, then $\mathcal{M}_1(d^1_{2k^*}, c^1_{k^*}) > 0$. By lemma 4.1(1), $\mathcal{M}_k(d^1_{2k^*}, c^1_{k^*}) > 0$ for any $k \notin \Gamma_1$. Hence, $\mathcal{P}_1(\lambda) = 0$ has a pair of purely imaginary roots, and for any $k \neq k^*$, $\mathcal{P}_k(\lambda) = 0$ has no zero eigenvalue.

Moreover, according to (4.15) and (4.22) the transversality conditions are fulfilled. Therefore, system (1.3) undergoes a $(k^*, 1)$-mode Turing–Hopf bifurcation near positive constant steady state E_* at $(d_2, c) = (d^1_{2k^*}, c^1_{k^*})$. □

https://doi.org/10.1017/prm.2024.24 Published online by Cambridge University Press

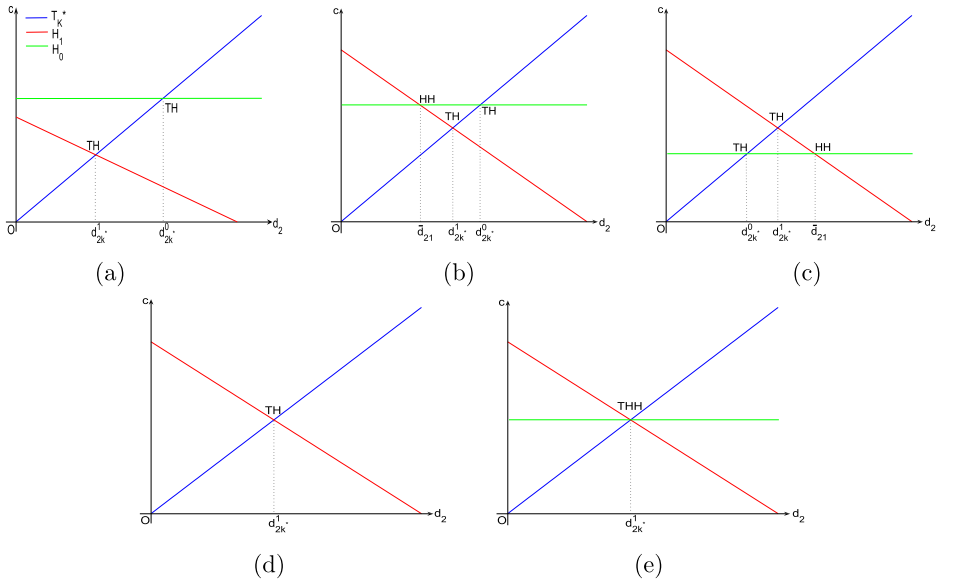

Figure 14. Turing–Hopf, double-Hopf, and Turing–double-Hopf bifurcations of system (1.3) near E_* in the (d_2, c)-plane for any $l > 0$: (a) $(a, b, e, u_*) \in U_{32}$ and $u_* l^2 \leqslant d_1 < s_1 l^2$; (b) $(a, b, e, u_*) \in U_{32}$, $0 < d_1 < u_* l^2$ and $d_{2k^*}^0 > \bar{d}_{21}$; (c) $(a, b, e, u_*) \in U_{32}$, $0 < d_1 < u_* l^2$ and $d_{2k^*}^0 < \bar{d}_{21}$; (d) $(a, b, e, u_*) \in U_{31}$; (e) $(a, b, e, u_*) \in U_{32}$ and $d_{2k^*}^0 = \bar{d}_{21}$. H_0, H_1, and T_{k^*} represent the 0-mode, 1-mode Hopf bifurcation, and k^*-mode Turing bifurcation curves, respectively. TH, HH, and THH represent Turing–Hopf bifurcation, double-Hopf bifurcation, and Turing–double-Hopf bifurcation, respectively.

REMARK 4.11. When $k^* = 1$, a Bogdanov–Takens bifurcation may occur. To reduce the length of the paper, we ignore the case $k^* = 1$.

THEOREM 4.12. *For any $l > 0$ and $(a, b, e, u_*) \in U_{32}$, assume that $0 < d_1 < s_1 l^2$, $k^* > 1$, and $c_{k_0}^T \neq c_{k_0+1}^T$, then the following statements hold:*

(1) *if $u_* l^2 \leqslant d_1 < s_1 l^2$, system (1.3) undergoes a $(k^*, 0)$-mode Turing–Hopf bifurcation near constant steady state E_* at $(d_{2k^*}^0, c_{k^*}^0)$.*

(2) *if $0 < d_1 < u_* l^2$, then we have the following result:*

   (i) *when $d_{2k^*}^0 > \bar{d}_{21}$, then system (1.3) undergoes a $(k^*, 0)$-mode Turing–Hopf bifurcation near constant steady state E_* at $(d_{2k^*}^0, c_{k^*}^0)$;*

   (ii) *when $d_{2k^*}^0 < \bar{d}_{21}$, then system (1.3) undergoes a $(k^*, 1)$-mode Turing–Hopf bifurcation near constant steady state E_* at $(d_{2k^*}^1, c_{k^*}^1)$.*

Moreover, the real parts of other eigenvalues for the characteristic equation (4.3) are negative except for a pair of purely imaginary eigenvalues and a simple zero eigenvalue. Here, $d_{2k^*}^1$, $d_{2k^*}^0$, $\bar{d}_{21}$, $c_{k^*}^1$, and $c_{k^*}^0$ are given in (4.13), (4.17), (4.20), and (4.23), respectively.

https://doi.org/10.1017/prm.2024.24 Published online by Cambridge University Press

Proof. (1) As $(a, b, e, u_*) \in U_{32}$, then $c_0^H > 0$. Let $c_0^H = c_{k^*}^H$, we obtain the intersection of H_0 and T_{k^*}, given by $(d_{2k^*}^0, c_{k^*}^0)$, and $(d_{2k^*}^0, c_{k^*}^0)$ is above $(d_{2k^*}^1, c_{k^*}^1)$ in the (d_2, c)-plane. When $(d_2, c) = (d_{2k^*}^0, c_{k^*}^0)$, $\mathcal{T}_0(d_{2k^*}^0, c_{k^*}^0) = 0$. If $u_* l^2 \leqslant d_1 < s_1 l^2$, then $\mathcal{T}_1(d_{2k^*}^0, c_{k^*}^0) = -v_* c_{k^*}^0 + s_1 - d_1/l^2 - d_{2k^*}^0/l^2 = u_* l^2 - d_1/l^2 - d_{2k^*}^0/l^2 < 0$. Since $\mathcal{T}_k$ is decreasing in k, then for any positive integer k, $\mathcal{T}_k(d_{2k^*}^0, c_{k^*}^0) \leqslant \mathcal{T}_1(d_{2k^*}^0, c_{k^*}^0) < 0$ hold, which implies that $\mathcal{T}_{k^*}(d_{2k^*}^0, c_{k^*}^0) < 0$. On the other hand, for $(d_2, c) = (d_{2k^*}^0, c_{k^*}^0)$, $\mathcal{M}_{k^*}(d_{2k^*}^0, c_{k^*}^0) = 0$. Hence, $\mathcal{P}_{k^*}(\lambda) = 0$ has a simple zero, and for any $k \neq 0$, $\mathcal{P}_k(\lambda) = 0$ has no purely imaginary roots.

For any $k \notin \Gamma_1$, by lemma 4.1(1), $\mathcal{M}_k(c) > 0$ for any $c > 0$, thus $\mathcal{M}_k(d_{2k^*}^0, c_{k^*}^0) > 0$, and we also have $\mathcal{M}_0(d_{2k^*}^0, c_{k^*}^0) > 0$. When $k^* > 1$ and $c_{k_0}^T \neq c_{k_0+1}^T$, by the definition of k^*, we have $c_{k^*}^0 = c_0^H = c_{k^*}^T(d_{2k^*}^0) \geqslant c_k^T(d_{2k^*}^0)$ for any $k \in \mathbb{N}$, then $\mathcal{M}_k(d_{2k^*}^0, c_{k^*}^0) > 0$ for $k \in \Gamma_1$ and $k \neq k^*$, which implies that $\mathcal{P}_0(\lambda) = 0$ has a pair purely imaginary roots, and for any $k \neq k^*$, $\mathcal{P}_k(\lambda) = 0$ has no zero eigenvalue. Moreover, the transversality conditions hold via (4.19) and (4.22). Hence, system (1.3) undergoes a $(k^*, 0)$-mode Turing–Hopf bifurcation at $(d_2, c) = (d_{2k^*}^0, c_{k^*}^0)$.

(2) If $0 < d_1 < u_* l^2$, then H_0 and H_1 intersect at $(d_2, c) = (\bar{d}_{21}, c_0^H)$. According to the relationship between $\bar{d}_{21}$ and $d_{2k^*}^0$, we have the following two cases:

(i) if $\bar{d}_{21} < d_{2k^*}^0$, then $(d_{2k^*}^0, c_{k^*}^0)$ is above $(d_{2k^*}^1, c_{k^*}^1)$ in the (d_2, c)-plane, see figure 14(b);

(ii) if $\bar{d}_{21} > d_{2k^*}^0$, then $(d_{2k^*}^0, c_{k^*}^0)$ is below $(d_{2k^*}^1, c_{k^*}^1)$ in the (d_2, c)-plane, see figure 14(c).

Case (2) can be proved by using the same argument as in the proofs of theorem 4.10 and case (1). □

Corollary 4.13. *For any $l > 0$ and $(a, b, e, u_*) \in U_{32}$, assume that $0 < d_1 < s_1 l^2$, $k^* > 1$, and $c_{k_0}^T \neq c_{k_0+1}^T$, then system (1.3) undergoes a $(k^*, 1, 0)$-mode Turing–double-Hopf bifurcation near the constant steady state E_* at $(d_{2k^*}^1, c_{k^*}^1)$, when $d_{2k^*}^0 = \bar{d}_{21}$. Moreover, the real parts of other eigenvalues for the characteristic equation (4.3) are negative except for two pairs of purely imaginary eigenvalues and a simple zero eigenvalue (see figure 14(e)).*

4.3. Spatiotemporal patterns via double-Hopf bifurcation

In this subsection, we use the formulas derived by Geng and Wang [**13**] to compute the (0, 1)-mode double-Hopf bifurcation normal form, which may help us to find some interesting spatiotemporal patterns. Let:

$$d_2 = \bar{d}_{21} + \eta_1, \quad c = c_0^H + \eta_2,$$

where $\bar{d}_{21}$ and c_0^H are given in (4.20) and (4.16), respectively. Define:

$$V(t) = (u(t), v(t))^T, \quad \hat{V}(t) = \frac{1}{l\pi} \int_0^{l\pi} V(y, t)\, \mathrm{d}y,$$

and system (1.3) can be transformed into:

$$\dot{V}(t) = D_0(\eta)\Delta V(t) + L(\eta)V(t) + \hat{L}(\eta)\hat{V}(t) + G(V(t), \hat{V}(t), \eta), \tag{4.24}$$

https://doi.org/10.1017/prm.2024.24 Published online by Cambridge University Press

in which

$$D(\eta)=\begin{pmatrix} d_1 & 0 \\ 0 & \bar{d}_{21}+\eta_1 \end{pmatrix},$$

$$L(\eta)=\begin{pmatrix} s_1 & -\dfrac{bu_*}{a+u_*} \\ \dfrac{aev_*}{(a+u_*)^2}c_0^H & -v_*c_0^H \end{pmatrix}, \quad \hat{L}(\eta)=\begin{pmatrix} -u_* & 0 \\ 0 & 0 \end{pmatrix},$$

$$G(\mathbf{u},\hat{\mathbf{u}},\eta)=\begin{pmatrix} (u+u_*)(1-\hat{u}-u_*)-\dfrac{b(u+u_*)(v+v_*)}{a+u+u_*}+u_*\hat{u}-s_1u_1+\dfrac{bu_*}{a+u_*}v \\ (c_0^H+\eta_2)(v+v_*)\left(1-v-v_*+\dfrac{e(u+u_*)}{a+u+u_*}\right)-(c_0^H+\eta_2)\left(\dfrac{aev_*}{(a+u_*)^2}u-v_*v\right) \end{pmatrix},$$

and $\mathbf{u}=(u,\,v)^T$, $\hat{\mathbf{u}}=(\hat{u},\,\hat{v})^T:=(1/l\pi)\int_0^{l\pi}\mathbf{u}(\zeta,\,t)\mathrm{d}\zeta$, $\eta=(\eta_1,\,\eta_2)$. Then

$$D_0(\eta)=\begin{pmatrix} d_1 & 0 \\ 0 & \bar{d}_{21} \end{pmatrix}, \quad D_1(\eta)=\begin{pmatrix} 0 & 0 \\ 0 & \eta_1 \end{pmatrix},$$

$$L_0=\begin{pmatrix} s_1 & -\dfrac{bu_*}{a+u_*} \\ \dfrac{aeu_*(1-u_*)}{(a+u_*)^2}c_0^H & -v_*c_0^H \end{pmatrix}, \quad L_1(\eta)=\begin{pmatrix} 0 & 0 \\ \dfrac{aeu_*}{(a+u_*)^2}\eta_2 & -v_*\eta_2 \end{pmatrix},$$

$$\hat{L}(0)(\eta)=\begin{pmatrix} -u_* & 0 \\ 0 & 0 \end{pmatrix}, \quad \hat{L}_1(\eta)=\begin{pmatrix} 0 & 0 \\ 0 & 0 \end{pmatrix},$$

$$Q(\mathbf{V},\mathbf{V})=\left(\frac{2a(1-u_*)}{(a+u_*)^2}u^2-\frac{2ab}{(a+u_*)^2}uv-2u_*u\hat{u}-\frac{2aev_*c_0^H}{(a+u_*)^3}u^2+\frac{2aec_0^H}{(a+u_*)^2}uv-2c_0^Hv^2\right),$$

$$C(\mathbf{V},\mathbf{V},\mathbf{V})=\begin{pmatrix} -\dfrac{6a(1-u_*)}{(a+u_*)^3}u^3+\dfrac{6ab}{(a+u_*)^3}u^2v \\ \dfrac{6aev_*c_0^H}{(a+u_*)^4}u^3-\dfrac{6aec_0^H}{(a+u_*)^3}u^2v \end{pmatrix},$$

where $\mathbf{V}=\begin{pmatrix}\mathbf{u}\\ \hat{\mathbf{u}}\end{pmatrix}$. For the (0, 1)-mode double-Hopf bifurcation, according to [13], the eigenfunctions ϕ_1, $\bar{\phi}_i$, ψ_1, $\bar{\psi}_i$ $(i=1,\,2)$ satisfying $\psi_i\phi_i=1$, $\psi_i\phi_j=1$ for i, $j=1,\,2$ $(j\neq i)$ are

$$\phi_1=\begin{pmatrix}1\\ \phi_{12}\end{pmatrix}, \quad \phi_2=\begin{pmatrix}1\\ \phi_{22}\end{pmatrix}, \quad \psi_1=\begin{pmatrix}\dfrac{1}{N_1}\\ \dfrac{\psi_{12}}{N_1}\end{pmatrix}^T, \quad \psi_2=\begin{pmatrix}\dfrac{1}{N_2}\\ \dfrac{\psi_{22}}{N_2}\end{pmatrix}^T,$$

https://doi.org/10.1017/prm.2024.24 Published online by Cambridge University Press

where

$$\phi_{12}=\frac{(a+u_*)(s_1-u_*-\mathrm{i}\omega_1)}{bu_*},\quad \phi_{22}=\frac{(a+u_*)(s_1-\mathrm{i}\omega_2-d_1/l^2)}{bu_*},$$
$$\psi_{12}=-\frac{bu_*}{(a+u_*)(\mathrm{i}\omega_1+c_0^H v_*)},\quad \psi_{22}=-\frac{bu_*}{(a+u_*)(\mathrm{i}\omega_2+c_0^H v_*+\bar{d}_{21}/l^2)},$$
$$N_1=1+\phi_{12}\psi_{12},\quad N_2=1+\phi_{22}\psi_{22}.$$

Next, we fix the parameters of (1.3) except d_2, c as follows:

$$a=0.5,\quad b=0.25,\quad e=5.9375,\quad d_1=0.5,\quad l=3.$$

For $(k_1, k_2)=(0, 1)$, according to Lemma 3.4 and Proposition 3.5 in [**13**], we have the following statements.

PROPOSITION 4.14. *For system* (1.3) *with* $(d_1, a, b, e, l)=(0.5, 0.5, 0.25, 5.9375, 3)$, *the positive constant steady state* E_* *is* $(0.125, 2.1875)$, *and there exist critical values* $(\bar{d}_{21}, c_0^H, \omega_1, \omega_2)\doteq(0.625, 0.02286, 0.1285, 0.03762)$ *such that when* $(d_2, c)=(\bar{d}_{21}, c_0^H)$, *all eigenvalues of* $\mathcal{P}_k(\lambda)$ *have negative real parts other than two pairs of purely imaginary roots* $\pm\mathrm{i}\omega_1$, $\pm\mathrm{i}\omega_2$, *and system* (1.3) *undergoes a* $(0, 1)$*-mode double-Hopf bifurcation near* E_*.

By Lemma 3.4 and Proposition 3.5 in [**13**], the coefficients of the normal form up to third order are as follows:

$$\begin{aligned}
&a_1(\eta)=-(1.09375-2.80989\mathrm{i})\eta_2,\\
&b_2(\eta)=-(0.055556+0.1756399\mathrm{i})\eta_1-(1.09375-7.57567\mathrm{i})\eta_2,\\
&a_{2100}=-1.28834-3.135\mathrm{i},\quad a_{1011}=-21.5985-41.8235\mathrm{i},\\
&b_{0021}=10.0251-6.5363\mathrm{i},\quad b_{1110}=28.6488+141.7397\mathrm{i},
\end{aligned}\tag{4.25}$$

by making the following transformations successively:

$$z_1=r_1\cos(\theta)+\mathrm{i}r_1\sin(\theta),\quad z_2=r_2\cos(\theta)+\mathrm{i}r_2\sin(\theta);$$
$$\sqrt{|\mathrm{Re}(a_{2100})|}\mathrm{sign}(\mathrm{Re}(a_{2100})r_1\to r_1,\ \sqrt{|\mathrm{Re}(b_{0021})|}r_2\to r_2,\ \mathrm{sign}(\mathrm{Re}(a_{2100}))t\to t,$$

then the corresponding planar system is

$$\begin{aligned}
\dot{r}_1&=r_1(1.09375\eta_2+r_1^2-2.1545r_2^2),\\
\dot{r}_2&=r_2(0.0555556\eta_1+1.09375\eta_2-22.237r_1^2-r_2^2),
\end{aligned}\tag{4.26}$$

and all equilibria of system (4.26) are

$$\begin{aligned}
&E_0=(0,0),\quad E_1=(\sqrt{-1.0938\eta_2},0),\ \text{for } \eta_2<0,\\
&E_2=(0,\sqrt{0.055556\eta_1+1.0938\eta_2}),\ \text{for } \eta_2>-0.050794\eta_1,\\
&E_3=(\sqrt{0.002447\eta_1+0.02582\eta_2},\sqrt{0.001136\eta_1+0.5197\eta_2}),\\
&\qquad\text{for } 0.002447\eta_1+0.02582\eta_2>0 \text{ and } 0.001136\eta_1+0.5197\eta_2>0.
\end{aligned}$$

https://doi.org/10.1017/prm.2024.24 Published online by Cambridge University Press

It follows from $\mathrm{Re}(a_{2100}) = -1.28834 < 0$ that the Case VIII of the unfolding in Chapter 7 of [16] occurs. The critical bifurcation lines in the (d_2, c)-plane are as follows:

$$\begin{aligned} &H_0 : c = c_0^H, \quad H_1 : c = c_0^H - 0.050794(d_2 - \bar{d}_{21}), \\ &L_1 : c = c_0^H - 0.09479(d_2 - \bar{d}_{21}), \quad d_2 < \bar{d}_{21}, \\ &L_2 : c = c_0^H - 0.002186(d_2 - \bar{d}_{21}), \quad d_2 > \bar{d}_{21}. \end{aligned} \tag{4.27}$$

As shown in figure 15(a), the (d_2, c)-plane is divided into six disjoint regions around $(\bar{d}_{21}, c_0^H)$, and the corresponding phase portraits are given in figure 15(b). The equilibria E_0, E_1, E_2, and E_3 of normal form system (4.26) corresponding to the positive constant steady state, the spatially homogeneous periodic solution, the spatially nonhomogeneous periodic solution, and spatially nonhomogeneous quasi-periodic solution of system (1.3), respectively. Thus, the dynamics of system (1.3) near the (0, 1)-mode double-Hopf bifurcation singularity in the (d_2, c)-plane can be classified as follows:

(1) When $(d_2, c) \in$ I, E_* is unstable.

(2) When $(d_2, c) \in$ II, E_* remain unstable, and an unstable spatially homogeneous periodic solution $\bar{E}_1$ bifurcates from E_*.

(3) When $(d_2, c) \in$ III, E_*, and the spatially homogeneous periodic solution $\bar{E}_1$ are unstable, and an unstable spatially nonhomogeneous periodic solution $\bar{E}_2$ appears.

(4) When $(d_2, c) \in$ IV, E_*, and the spatially homogeneous periodic solution $\bar{E}_1$ are unstable, the spatially nonhomogeneous periodic solution $\bar{E}_2$ becomes locally asymptotically stable, and an unstable spatially nonhomogeneous quasi-periodic solution $\bar{E}_3$ appears.

(5) When $(d_2, c) \in$ V, E_* becomes locally asymptotically stable, the spatially homogeneous periodic solution $\bar{E}_2$ becomes unstable, the quasi-periodic solution $\bar{E}_3$ remain unstable, and there is no spatially homogeneous periodic solution $\bar{E}_1$.

(6) When $(d_2, c) \in$ VI, E_* remains locally asymptotically stable, the spatially nonhomogeneous quasi-periodic solution $\bar{E}_3$ disappears, and the spatially nonhomogeneous periodic solution $\bar{E}_2$ still unstable.

5. Concluding remarks

In this paper, we formulated and rigorously studied a host–parasitoid model with generalist predation and diffusion, where the predators have alternative food. After performing a detailed bifurcation analysis, our results revealed that system (1.3) exhibits complex dynamics and rich bifurcations. For a local model, we provided some preliminary analysis on Hopf bifurcation. For a reaction–diffusion model with local intraspecific prey competition, we first obtained the Turing instability

https://doi.org/10.1017/prm.2024.24 Published online by Cambridge University Press

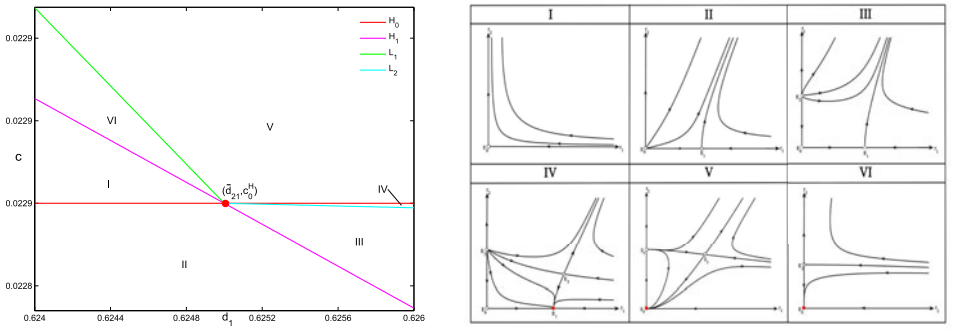

(a) (b)

Figure 15. (a) Bifurcation set of system (4.26) near $(\bar{d}_{21}, c_0^H)$ in the (d_2, c)-plane. (b) The corresponding phase portraits in I–VI, where H_0, H_1, L_1, and L_2 represent critical bifurcation curves defined as in (4.27).

of spatially homogeneous steady states or spatially homogeneous periodic solutions. Then, we showed that the model with diffusion undergoes Hopf bifurcation and Turing–Hopf bifurcation. Especially, we found two different normal forms for the Turing–Hopf bifurcation, where a pair of spatially nonhomogeneous periodic solutions is stable for a (8,0)-mode Turing–Hopf bifurcation and unstable for a (3,0)-mode Turing–Hopf bifurcation. Our results indicate that the model exhibits complex pattern formations, including transient states (spatially homogeneous or nonhomogeneous periodic solutions), monostability (a spatially nonhomogeneous steady state or a spatially homogeneous periodic solution), bistability (a pair of spatially nonhomogeneous steady states or a pair of spatially nonhomogeneous periodic solutions), tristability (a pair of spatially nonhomogeneous steady states and a spatially homogeneous periodic solution), and heteroclinic orbits (connecting a spatially nonhomogeneous periodic solution to a non-constant steady state or a spatially homogeneous periodic solution, connecting a spatially homogeneous periodic solution to non-constant steady states and vice versa). Finally, numerical simulations are provided to illustrate complex dynamics and verify our theoretical results.

It is worth noting that we found two kinds of normal forms with different dynamics for Turing–Hopf bifurcation (see § 3), i.e. the (8,0)-mode Turing–Hopf bifurcation with a pair of stable spatially nonhomogeneous periodic solutions, and the (3,0)-mode Turing–Hopf bifurcation with a pair of unstable spatially nonhomogeneous periodic solutions. These two are similar to the Cases Ia and Ib in section 7.5 of [**16**]. Recently, although Turing–Hopf bifurcation and the corresponding spatiotemporal patterns are discussed in different systems (see [**5**, **19**, **24**, **32**, **41**] and references therein), normal forms with different modes having different dynamics for Turing–Hopf bifurcation in an applied problem are rare (see [**19**, **20**]).

After replacing the local intraspecific prey competition by nonlocal intraspecific prey competition in diffusion model (1.3), we obtained more complex dynamics, such as (i) both $(k, 0)$-mode and $(k, 1)$-mode Turing–Hopf bifurcations can destabilize the constant equilibrium E^*, whereas in contrast only $(k, 0)$-mode for

https://doi.org/10.1017/prm.2024.24 Published online by Cambridge University Press

system with local interactions; (2) nonlocal interaction can induce double-Hopf and Turing–double-Hopf bifurcations, while local interaction cannot; (3) when $k^* = 1$, a 1-mode Bogdanov–Takens bifurcation may occur; and (4) double-Hopf bifurcation can induce a superposition of time-periodic solutions with different spatial modes.

The spatially nonhomogeneous periodic solutions are stable for some parameter values (according to the result of the (8,0)-mode Turing–Hopf bifurcation) and unstable for other parameter values (according to the result of the (3,0)-mode Turing–Hopf bifurcation), which implies that system (1.3) may have a degenerate spatially nonhomogeneous Hopf bifurcation around E_*. Moreover, our results in [**38**] showed that the local system of (1.3) exhibits degenerate Hopf bifurcation with codimension up to 2 at E_*, then we can discuss Turing instability of degenerate spatially homogeneous periodic solutions. We leave these as open questions.

Acknowledgements

Research was partially supported by NSFC (No. 12231008), NSERC (RGPIN-2020-03911 and RGPAS-2020-00090) and NSF (DMS-2052648).

References

1 F. Andreu-Vaillo, J. M. Mazon, J. D. Rossi and J. J. Toledo-Melero, *Nonlocal Diffusion Problems*, Mathematical Surveys and Monographs, Vol. 165 (American Mathematical Society, Providence, RI, 2010).

2 P. W. Bates, On some nonlocal evolution equations arising in materials science, in 'Nonlinear Dynamics and Evolution Equations', H. Brunner, X.-Q. Zhao and X. Zou (eds.), Fields Institute Communications **48** (2006), 13–52.

3 N. F. Britton. Aggregation and the competitive exclusion principle. *J. Theor. Biol.* **136** (1989), 57–66.

4 R. S. Cantrell and C. Cosner, *Spatial Ecology via Reaction–Diffusion Equations*, Wiley Series in Mathematical and Computational Biology (John Wiley & Sons, 2003).

5 X. Cao and W. Jiang. Turing–Hopf bifurcation and spatiotemporal patterns in a diffusive predator–prey system with Crowley–Martin functional response. *Nonlinear Anal. Real World Appl.* **43** (2018), 428–450.

6 X. Cao and W. Jiang. Double zero singularity and spatiotemporal patterns in a diffusive predator–prey model with nonlocal prey competition. *Discrete Contin. Dyn. Syst. Ser. B* **25** (2020), 3461–3489.

7 S. Chen and J. Yu. Stability and bifurcation in predator–prey systems with nonlocal prey competition. *Discrete Contin. Dyn. Syst.* **38** (2018), 43–61.

8 Y. Du and Y. Lou. Qualitative behavior of positive solutions of a predator–prey model: effects of saturation. *Proc. R. Soc. Edinburgh Sect. A* **131** (2001), 321–349.

9 A. Erbach, F. Lutscher and G. Seo. Bistability and limit cycles in generalist predator–prey dynamics. *Ecol. Complex* **14** (2013), 48–55.

10 G. B. Ermentrout and J. D. Cowan. Secondary bifurcation in neuronal nets. *SIAM J. Appl. Math.* **39** (1980), 323–340.

11 W. F. Fagan, M. A. Lewis, M. G. Neubert and P. Van Den Driessche. Invasion theory and biological control. *Ecol. Lett.* **5** (2002), 148–157.

12 J. Furter and M. Grinfeld. Local vs. nonlocal interactions in population dynamics. *J. Math. Biol.* **27** (1989), 65–80.

13 D. Geng and B. Wang. Normal form formulations of double-Hopf bifurcation for partial functional differential equations with nonlocal effect. *J. Differ. Equ.* **309** (2022), 741–785.

14 S. Gourley. Travelling front solutions of a nonlocal Fisher equation. *J. Math. Biol.* **41** (2000), 272–284.

15 S. Gourley and S. Ruan. Spatio-temporal delays in plankton models: local stability and bifurcations. *Appl. Math. Comput.* **145** (2003), 391–412.

https://doi.org/10.1017/prm.2024.24 Published online by Cambridge University Press

16 J. Guckenheimer and P. Holmes. *Nonlinear Oscillations, Dynamical Systems, and Bifurcations of Vector Fields* (New York, Springer, 1983).
17 I. Hanski, L. Hansson and H. Henttonen. Specialist predators, generalist predators and the microtine rodent cycle. *J. Anim. Ecol.* **60** (1991), 353–367.
18 B. D. Hassard, N. D. Kazarinoff and Y. H. Wan. *Theory and Application for Hopf Bifurcation* (Cambridge, Cambridge University Press, 1981).
19 W. Jiang, Q. An and J. Shi. Formulation of the normal form of Turing–Hopf bifurcation in partial functional differential equations. *J. Differ. Equ.* **268** (2020), 6067–6102.
20 W. Jiang, H. Wang and X. Cao. Turing instability and Turing–Hopf bifurcation in diffusive Schnakenberg system with gene expression time delay. *J. Dyn. Differ. Equ.* **31** (2019), 2223–2247.
21 T. Lindström. Qualitative analysis of a predator–prey system with limit cycles. *J. Math. Biol.* **31** (1993), 541–561.
22 Z. Liu, Z. Shen, H. Wang and Z. Jin. Analysis of a diffusive SIR model with seasonality and nonlocal incidence of infections. *SIAM J. Appl. Math.* **79** (2019), 2218–2241.
23 M. Lu, J. Huang and H. Wang. An organizing center of codimension four in a predator–prey model with generalist predator: from tristability and quadristability to transients in a nonlinear environmental change. *SIAM J. Appl. Dyn. Syst.* **22** (2023), 694–729.
24 M. Lu, C. Xiang, J. Huang and H. Wang. Bifurcations in the diffusive Bazykin model. *J. Differ. Equ.* **323** (2022), 280–311.
25 S. Madec, J. Casas, G. Barles and C. Suppo. Bistability induced by generalist natural enemies can reverse pest invasions. *J. Math. Biol.* **75** (2017), 543–575.
26 C. Magal, C. Conser, S. Ruan and J. Casas. Control of invasive hosts by generalist parasitoids. *Math. Med. Biol.* **25** (2008), 1–20.
27 M. R. Owen and M. A. Lewis. How predation can slow, stop or reverse a prey invasion. *Bull. Math. Biol.* **63** (2001), 655–684.
28 L. Perko. *Differential Equations and Dynamical Systems* (3rd ed., New York, Springer, 2006).
29 S. Ruan, Spatial–temporal dynamics in nonlocal epidemiological models, in 'Mathematics for Life Science and Medicine', Y. Takeuchi, K. Sato, and Y. Iwasa (eds.), (Springer-Verlag, Berlin, 2007, pp. 97–122).
30 S. J. Schreiber. On coexistence of species sharing a predator. *J. Differ. Equ.* **196** (2004), 209–225.
31 G. Seo and G. S. K. Wolkowicz. Pest control by generalist parasitoids: a bifurcation theory. *Discrete Contin. Dyn. Syst. Ser. S* **13** (2020), 3157–3187.
32 H. Shi and S. Ruan. Spatial, temporal and spatiotemporal patterns of diffusive predator–prey models with mutual interference. *IMA J. Appl. Math.* **80** (2015), 1534–1568.
33 J. Shi, C. Wang and H. Wang. Diffusive spatial movement with memory and maturation delays. *Nonlinearity* **32** (2019), 3188–3208.
34 G. Sun, H. Zhang, L. Chang, Z. Jin, H. Wang and S. Ruan. On the dynamics of a diffusive foot-and-mouth disease model with nonlocal infections. *SIAM J. Appl. Math.* **82** (2022), 1587–1610.
35 E. van Leeuwen, V. A. A. Jansen and P. W. Bright. How population dynamics shape the functional response in a one-predator–two-prey system. *Ecology* **88** (2007), 1571–1581.
36 H. Wang and Y. Salmaniw. Open problems in PDE models for knowledge-based animal movement via nonlocal perception and cognitive mapping. *J. Math. Biol.* **86** (2023), 71.
37 S. Wu and Y. Song. Stability and spatiotemporal dynamics in a diffusive predator–prey model with nonlocal prey competition. *Nonlinear Anal. Real World Appl.* **48** (2019), 12–39.
38 C. Xiang, J. Huang, S. Ruan and D. Xiao. Bifurcation analysis in a host–generalist parasitoid model with Holling II functional response. *J. Differ. Equ.* **268** (2020), 4618–4662.
39 C. Xiang, J. Huang and H. Wang. Linking bifurcation analysis of Holling–Tanner model with generalist predator to a changing environment. *Stud. Appl. Math.* **149** (2022), 124–163.
40 D. Xiao and K. F. Zhang. Multiple bifurcations of a predator–prey system. *Discrete Contin. Dyn. Syst. Ser. B* **8** (2007), 417–437.

41 R. Yang and Y. Song. Spatial resonance and Turing–Hopf bifurcations in the Gierer–Meinhardt model. *Nonlinear Anal. Real World Appl.* **31** (2016), 356–387.

42 F. Yi, J. Wei and J. Shi. Bifurcation and spatiotemporal patterns in a homogeneous diffusive predator–prey system. *J. Differ. Equ.* **246** (2009), 1944–1977.

43 G. Zhao and S. Ruan. Spatial and temporal dynamics of a nonlocal viral infection model. *SIAM J. Appl. Math.* **78** (2018), 1954–1980.

https://doi.org/10.1017/prm.2024.24 Published online by Cambridge University Press